Mixed-Metal Cluster Chemistry. 22. Synthesis and Crystallographic, Electrochemical, and Theoretical Studies of Alkyne-Coordinated Group 6−Iridium Clusters Linked by Phenyleneethynylene Groups

Nigel T. Lucas, Eleni G. A. Notaras, Simon Petrie, Robert Stranger, and Mark G. Humphrey*

Department of Chemistry, Australian National University, Canberra ACT 0200, Australia

Received November 4, 2002

Reaction between the tetrahedral cluster compound $Mo_2Ir_2(CO)_{10}(\eta^5\text{-}C_5H_4Me)_2$ (**1**) and 1-iodo-4-(oct-1′-ynyl)benzene afforded the pseudooctahedral cluster $Mo_2Ir_2\{\mu_4\text{-}\eta^2\text{-}Me(CH_2)_5C_2\text{-}4\text{-}C_6H_4I\}(CO)_8(\eta^5\text{-}C_5H_4Me)_2$ (**7**). Similar reactions of **1** and $W_2Ir_2(CO)_{10}(\eta^5\text{-}C_5H_4Me)_2$ (**2**) with di- and triynes afforded the related mono-, di-, and tricluster compounds $[M_2Ir_2(CO)_8(\eta^5\text{-}C_5H_4Me)_2]_3\{\mu_{12}\text{-}\eta^6\text{-}Me(CH_2)_5C_2\text{-}4\text{-}C_6H_4C_2C_6H_4\text{-}4\text{-}C_2(CH_2)_5Me\}$ (M = Mo (**12**), W (**14**)), $[W_2Ir_2(CO)_8(\eta^5\text{-}C_5H_4Me)_2]_2\{\mu_8\text{-}\eta^4\text{-}Me(CH_2)_5C_2\text{-}4\text{-}C_6H_4C_2C_6H_4\text{-}4\text{-}C\equiv C(CH_2)_5Me\}$ (**13**), $Mo_2Ir_2\{\mu_4\text{-}\eta^2\text{-}Me(CH_2)_5C_2C_6H_3\text{-}3,5\text{-}[C\equiv C(CH_2)_5Me]_2\}(CO)_8(\eta^5\text{-}C_5H_4Me)_2$ (**15**), and $[Mo_2Ir_2(CO)_8(\eta^5\text{-}C_5H_4Me)_2]_2\{\mu_8\text{-}\eta^4\text{-}[Me(CH_2)_5C_2]_2\text{-}1,3\text{-}C_6H_3\text{-}5\text{-}C\equiv C(CH_2)_5Me\}$ (**16**). Compound **13** corresponds to the 1,2-dicluster adduct of the linear triyne $Me(CH_2)_5C\equiv C\text{-}4\text{-}C_6H_4C\equiv C\text{-}4\text{-}C_6H_4C\equiv C(CH_2)_5Me$. No 1,3-dicluster isomer was isolated from direct reaction, but the related molybdenum-containing 1,3-dicluster isomer was prepared by exploiting organic reaction chemistry on precoordinated functionalized alkyne ligands. Thus, Sonogashira coupling of **7** with $Me_3SiC\equiv CH$ and subsequent desilylation afforded $Mo_2Ir_2\{\mu_4\text{-}\eta^2\text{-}Me(CH_2)_5C_2\text{-}4\text{-}C_6H_4C\equiv CR\}(CO)_8(\eta^5\text{-}C_5H_4Me)_2$ (R = $SiMe_3$ (**8**), H (**9**)). Sonogashira coupling of **7** and **9** gave the 1,3-isomer $[Mo_2Ir_2(CO)_8(\eta^5\text{-}C_5H_4Me)_2]_2\{\mu_8\text{-}\eta^4\text{-}Me(CH_2)_5C_2\text{-}4\text{-}C_6H_4C\equiv CC_6H_4\text{-}4\text{-}C_2(CH_2)_5Me\}$ (**18**), as well as the homocoupling product $[Mo_2Ir_2(CO)_8(\eta^5\text{-}C_5H_4Me)_2]_2\{\mu_8\text{-}\eta^4\text{-}Me(CH_2)_5C_2\text{-}4\text{-}C_6H_4C\equiv CC\equiv CC_6H_4\text{-}4\text{-}C_2(CH_2)_5Me\}$ (**19**); the identity of the latter was confirmed by a single-crystal X-ray diffraction study. Cyclic voltammetric scans for **12**−**14**, **18**, and **19** all show a reversible/quasi-reversible oxidation followed by an irreversible oxidation process. Compounds **18** and **19** (in which clusters are linked by long unsaturated bridges) exhibit one irreversible reduction process, whereas **12**−**14** (in which *n* cluster cores are linked by a phenylene unit) show *n* irreversible reduction processes. Density functional calculations indicate that oxidation and reduction both proceed with retention of the pseudooctahedral core geometry but that loss of a carbonyl ligand concomitant with two-electron reduction is energetically accessible, suggesting that this accounts for the irreversibility of the reduction step.

Introduction

Transition-metal carbonyl cluster chemistry has been of enduring interest.[1,2] The redox properties of clusters have been of particular interest, clusters having been subjected to numerous detailed electrochemical studies.[3−9] A natural extension to these studies is to link

electroactive cluster modules through unsaturated bridges and utilize electrochemical techniques to assess electronic communication,[10−22] but few examples of

---

* To whom correspondence should be addressed. Tel: +61 2 6125 2927. Fax: +61 2 6125 0760. E-mail: Mark.Humphrey@anu.edu.au.

(1) Shriver, D. F.; Kaesz, H. D.; Adams, R. D. *The Chemistry of Metal Cluster Complexes*; VCH: Weinheim, Germany, 1990.
(2) Braunstein, P.; Oro, L. A.; Raithby, P. R. *Metal Clusters in Chemistry*; Wiley-VCH: Weinheim, Germany, 1999.
(3) Lemoine, P. *Coord. Chem. Rev.* **1982**, *47*, 55.
(4) Geiger, W. E.; Connelly, N. G. *Adv. Organomet. Chem.* **1985**, *24*, 87.
(5) Lemoine, P. *Coord. Chem. Rev.* **1988**, *83*, 169.
(6) Drake, S. R. *Polyhedron* **1990**, *9*, 455.
(7) Zanello, P. In *Structure and Bonding*; Clarke, M. J., Goodenough, J. B., Jørgensen, C. K., Neilands, J. B., Reinen, D., Weiss, R., Eds.; Springer: Berlin, 1992; Vol. 79, p 101.
(8) Zanello, P. In *Stereochemistry of Organometallic and Inorganic Compounds*; Zanello, P., Ed.; Elsevier: Amsterdam, 1994; Vol. 5, p 181.

(9) Zanello, P.; de Biani, F. F. In *Metal Clusters in Chemistry*; Braunstein, P., Oro, L. A., Raithby, P. R., Eds.; Wiley-VCH: Weinheim, Germany, 1999; Vol. 2, p 1104.
(10) Worth, G. H.; Robinson, B. H.; Simpson, J. *Organometallics* **1992**, *11*, 3863.
(11) Osella, D.; Gambino, O.; Nevi, C.; Ravera, M.; Bertolino, D. *Inorg. Chim. Acta* **1993**, *206*, 155.
(12) Elder, S. M.; Robinson, B. H.; Simpson, J. *J. Organomet. Chem.* **1990**, *398*, 165.
(13) Fritch, J. R.; Vollhardt, K. P. C. *Angew. Chem., Int. Ed. Engl.* **1980**, *19*, 559.
(14) Worth, G. H.; Robinson, B. H.; Simpson, J. *Organometallics* **1992**, *11*, 501.
(15) Dellaca, R. J.; Penfold, B. R.; Robinson, B. H.; Robinson, W. T.; Spencer, J. L. *Inorg. Chem.* **1970**, *9*, 2204.
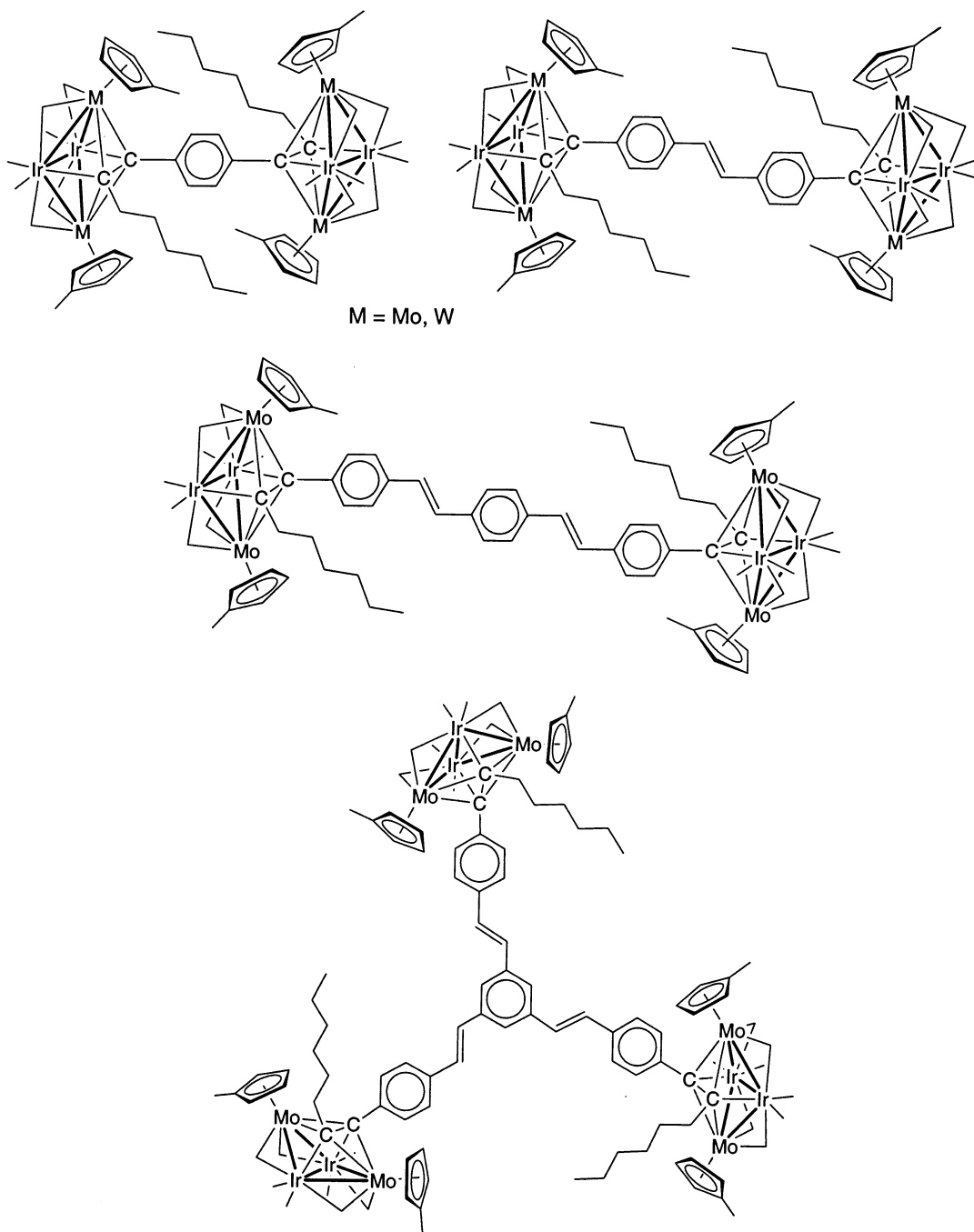(16) Dellaca, R. J.; Penfold, B. R. *Inorg. Chem.* **1971**, *10*, 1269.
(17) Bruce, M. I.; Williams, M. L.; Patrick, J. M.; White, A. H. *J. Chem. Soc., Dalton Trans.* **1985**, 1229.
(18) Adams, C. J.; Bruce, M. I.; Horn, E.; Skelton, B. W.; Tiekink, E. R. T.; White, A. H. *J. Chem. Soc., Dalton Trans.* **1993**, 3299.
(19) Daran, J.-C.; Cabrera, E.; Bruce, M. I.; Williams, M. L. *J. Organomet. Chem.* **1987**, *319*, 239.

Chart 1

M = Mo, W

heterometallic clusters linked by unsaturated bridges exist,[23–25] and until our recent report none had been examined electrochemically. As part of a detailed study of group 6–iridium mixed-metal cluster chemistry,[26–34]

we recently reported examples of cluster–alkyne adducts linked by phenylenevinylene bridges (Chart 1) and their examination by cyclic voltammetry and UV–vis–near-IR spectroelectrochemistry.[34] We have now ex-

(20) Wong, W. Y.; Cheung, S. H.; Lee, S. M.; Leung, S. Y. *J. Organomet. Chem.* **2000**, *596*, 36.

(21) Osella, D.; Hanzlik, J. *Inorg. Chim. Acta* **1993**, *213*, 311.

(22) Osella, D.; Gambino, O.; Nervi, C.; Ravera, M.; Russo, M. V.; Infante, G. *Gazz. Chim. Ital.* **1993**, *123*, 579.

(23) Bruce, M. I.; Halet, J.-F.; Kahlal, S.; Low, P. J.; Skelton, B. W.; White, A. H. *J. Organomet. Chem.* **1999**, *578*, 155.

(24) Jensen, M. P.; Phillips, D. A.; Sabat, M.; Shriver, D. F. *Organometallics* **1992**, *11*, 1859.

(25) Imhof, D.; Burckhardt, U.; Dahmen, K.-H.; Joho, F.; Nesper, R. *Inorg. Chem.* **1997**, *36*, 1813.

(26) Lee, J.; Humphrey, M. G.; Hockless, D. C. R.; Skelton, B. W.; White, A. H. *Organometallics* **1993**, *12*, 3468.

(27) Waterman, S. M.; Humphrey, M. G.; Tolhurst, V.-A.; Skelton, B. W.; White, A. H.; Hockless, D. C. R. *Organometallics* **1996**, *15*, 934.

(28) Waterman, S. M.; Humphrey, M. G.; Hockless, D. C. R. *Organometallics* **1996**, *15*, 1745.

(29) Waterman, S. M.; Humphrey, M. G. *Organometallics* **1999**, *18*, 3116.

(30) Waterman, S. M.; Humphrey, M. G.; Tolhurst, V.-A.; Bruce, M. I.; Low, P. J.; Hockless, D. C. R. *Organometallics* **1998**, *17*, 5789.

(31) Waterman, S. M.; Humphrey, M. G.; Lee, J.; Ball, G. E.; Hockless, D. C. R. *Organometallics* **1999**, *18*, 2440.

(32) Lucas, N. T.; Humphrey, M. G.; Rae, A. D. *Macromolecules* **2001**, *34*, 6188.

(33) Lucas, N. T.; Blitz, J. P.; Petrie, S.; Stranger, R.; Humphrey, M. G.; Heath, G. A.; Otieno-Alego, V. *J. Am. Chem. Soc.* **2002**, *124*, 5139.

(34) Lucas, N. T.; Notaras, E. G. A.; Cifuentes, M. P.; Humphrey, M. G. *Organometallics* **2003**, *22*, 284.
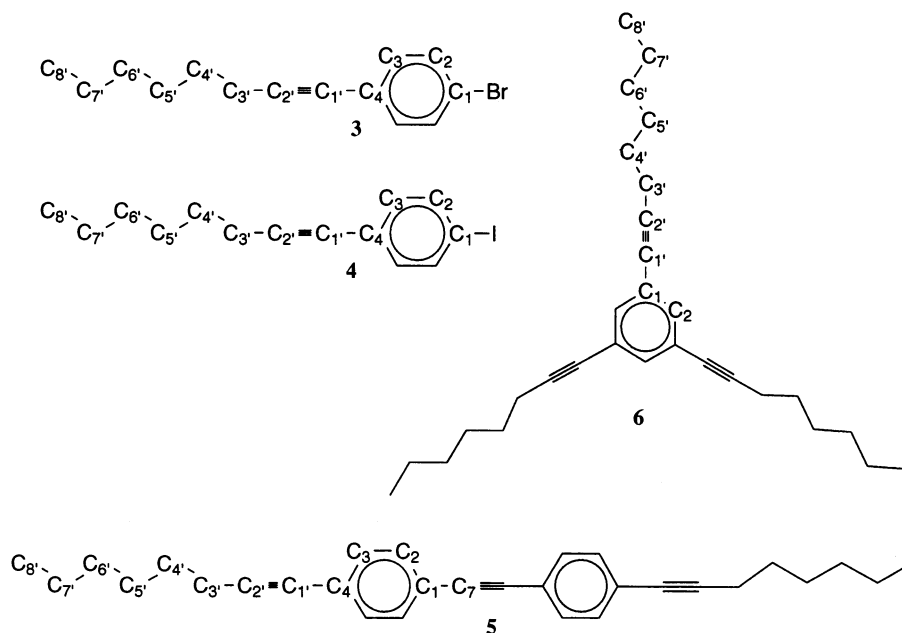
Figure 1. ^{1}H and ^{13}C NMR numbering schemes.

panded these studies to embrace bridging groups containing phenyleneethynylene units, the results from which are reported herein. Also reported in this account are theoretical studies on a model system which have been undertaken to rationalize the electrochemical behavior observed experimentally.

Experimental Section

General Conditions. Reactions were carried out under an atmosphere of argon or nitrogen using standard Schlenk techniques.[35] All cluster complexes except **9** proved to be indefinitely stable in air as solids and for at least short periods of time in solution, and thus no precautions were taken to exclude air in their manipulation. Tetrahydrofuran was laboratory reagent (LR) grade. All other solvents used were analytical reagent (AR) grade. Unless stated otherwise, the following reaction solvents were dried and distilled under argon using standard methods: CH_2Cl_2 over CaH_2; THF over sodium benzophenone ketyl. Triethylamine was used without drying but was purged with nitrogen prior to use. Solvents used in the workup (including chromatography and crystallizations) were used as received. Petroleum spirit refers to a petroleum fraction of boiling range 60−80 °C. Column chromatography was performed using Merck silica gel 60 of particle size 0.040−0.063 mm (230−400 mesh ASTM). The cluster products were purified by thin-layer chromatography (TLC) on 20 × 20 cm glass plates coated with Merck silica gel 60 PF_{254} (0.5 mm). Analytical TLC, used for monitoring the extent of reactions, was carried out on Merck aluminum sheets coated with 0.25 mm silica gel 60 PF_{254} and visualized under UV light (for colorless compounds).

Starting Materials and Reagents. The reagents 1-octyne, 4-bromo-1-iodobenzene, 1,3,5-tribromobenzene, (trimethylsilyl)acetylene, and *tert*-butyllithium solution (Aldrich), copper-(I) iodide (Unilab), iodine (M&B), and potassium carbonate (BDH) were purchased commercially and used as received. Literature procedures (or minor variations thereof) were used to synthesize dichlorobis(triphenylphosphine)palladium(II),[36] bis(4-bromophenyl)ethyne,[37] $Mo_2Ir_2(CO)_{10}(\eta^5\text{-}C_5H_4Me)_2$ (**1**),[33]

and $W_2Ir_2(CO)_{10}(\eta^5\text{-}C_5H_4Me)_2$ (**2**).[38] The *tert*-butyllithium (nominally 1.7 M in heptane) was titrated with diphenylacetic acid in THF prior to use to determine its exact concentration.[39]

Instruments. Infrared spectra were recorded on a Perkin-Elmer System 2000 FT-IR spectrometer in a solution cell with CaF_2 windows; spectral frequencies are recorded in cm^{-1}. All analytical spectra were recorded as solutions in either cyclohexane or CH_2Cl_2 (both AR grade). UV−vis spectra were recorded using a Cary 5G spectrophotometer as solutions in THF in 1 cm quartz cells, recorded over the range 240−1000 nm, and are reported in the form λ_{max} (ϵ). ^{1}H and ^{13}C NMR spectra were recorded in CDCl$_3$ (Cambridge Isotope Laboratories) using a Varian Gemini-300 spectrometer (^{1}H at 300 MHz; ^{13}C at 75 MHz, broadband proton decoupled). Spectra are referenced to residual CHCl$_3$ at 7.24 ppm (^{1}H) or CDCl$_3$ at 77.0 ppm (^{13}C). The assignments of the organic compounds follow the numbering schemes shown in Figure 1. Electron impact (EI) mass spectra (unit resolution and high resolution (HR)) were recorded using a VG Autospec instrument (70 eV electron energy, 8 kV accelerating potential) at the Research School of Chemistry, Australian National University. Secondary ion mass spectrometry (SIMS) spectra were recorded using a VG ZAB 2SEQ instrument (30 kV Cs$^+$ ions, current 1 mA, accelerating potential 8 kV, 3-nitrobenzyl alcohol matrix, solutions in CH_2Cl_2) at the Research School of Chemistry, Australian National University, or the Department of Chemistry, University of Western Australia. Fast-atom bombardment (FAB) mass spectra were recorded at the University of Bristol, Bristol, U.K., using a VG Autospec mass spectrometer (Ar source with accelerating potential of 6−8 kV, 3-nitrobenzyl alcohol matrix, solutions in CH_2Cl_2). All MS were calculated with the m/z value based on ^{79}Br, ^{96}Mo, ^{183}W, and ^{192}Ir assignments and are reported in the form m/z (assignment, relative intensity). Elemental microanalyses were carried out by the Microanalysis Service Unit in the Research School of Chemistry, Australian National University.

Synthesis of 1-Bromo-4-(oct-1′-ynyl)benzene (3). A solution of 4-bromo-1-iodobenzene (2.54 g, 8.98 mmol) in triethylamine (80 mL) was cooled to 0 °C, and 1-octyne (1.45 mL, 9.83 mmol), dichlorobis(triphenylphosphine)palladium(II) (64

(35) Shriver, D. F.; Drezdzon, M. A. *The Manipulation of Air-Sensitive Compounds*, 2nd ed.; Wiley: New York, 1986.
(36) Heck, R. F. *Palladium Reagents in Organic Syntheses*; Academic Press: London, England, 1985.

(37) Manna, J.; Kuehl, C. J.; Whiteford, J. A.; Stang, P. J. *Organometallics* **1997**, *16*, 1897.
(38) Lucas, N. T.; Notaras, E. G. A.; Humphrey, M. G. *Acta Crystallogr., Sect. E* **2001**, *57*, m132.
(39) Kofron, W. G.; Baclowski, L. M. *J. Org. Chem.* **1976**, *41*, 1879.

mg, 91 μmol), and copper(I) iodide (38 mg, 200 μmol) were added. After the mixture was stirred at 0 °C for 10 min, the ice bath was removed and the mixture stirred a further 2 h while it was warmed to room temperature. The triethylammonium iodide precipitate was removed by filtration through a sintered-glass funnel, and the filtrate was reduced to dryness in vacuo. The residue was dissolved in petroleum spirit (5 mL) and transferred to a short silica column which was eluted with petroleum spirit/dichloromethane (9/1). The solvent was removed from the eluant using a rotary evaporator, affording a colorless oil which was identified as 1-bromo-4-(oct-1′-ynyl)-benzene (**3**; 2.14 g, 8.05 mmol, 90%). IR (cyclohexane): ν(C≡C) 2229 w cm^{-1}. ^{1}H NMR (CDCl$_3$): δ 7.38 (d, J_{HH} = 9 Hz, 2H, H$_2$), 7.23 (d, J_{HH} = 9 Hz, 2H, H$_3$), 2.36 (t, J_{HH} = 7 Hz, 2H, H$_3'$), 1.57−1.30 (m, 8H, H$_4'$−H$_7'$), 0.88 (t, J_{HH} = 7 Hz, 3H, H$_8'$). ^{13}C NMR (CDCl$_3$): δ 133.0, 131.4 (C$_2$, C$_3$), 123.1, 121.5 (C$_4$, C$_1$), 91.8 (C$_1'$), 79.6 (C$_2'$), 31.3 (C$_3'$), 28.6 (C$_4'$, C$_5'$), 22.5 (C$_6'$), 19.4 (C$_7'$), 14.1 (C$_8'$). MS (EI): 264 ([M]$^+$, 66), 249 ([M − Me]$^+$, 2), 235 ([M − C$_2$H$_5$]$^+$, 18), 221 ([M − C$_3$H$_7$]$^+$, 52), 207 ([M − C$_4$H$_9$]$^+$, 10), 193 ([M − C$_5$H$_{11}$]$^+$, 62), 156 ([M − Br − C$_2$H$_5$]$^+$, 57), 142 ([M − Br − C$_3$H$_7$]$^+$, 98), 128 ([M − Br − C$_4$H$_9$]$^+$, 83), 116 ([M − Br − C$_5$H$_9$)]$^+$, 100). HR-MS (EI): calcd for C$_{14}$H$_{17}$-Br, 264.0514; found, 264.0513.

Synthesis of 1-Iodo-4-(oct-1′-ynyl)benzene (4). A stirred solution of 1-bromo-4-(oct-1′-ynyl)benzene (**3**; 2.13 g, 8.03 mmol) in THF (70 mL) was cooled to −77 °C and a solution of *tert*-butyllithium (12.0 mL, 1.35 M, 16.2 mmol) was added slowly. After 10 min of stirring at −77 °C, a solution of iodine (2.82 g, 11.1 mmol) in THF (15 mL) was added until a dark brown color persisted. The reaction mixture was warmed to room temperature over 30 min and then was transferred to a 250 mL separating funnel. The contents of the flask were rinsed into the separating funnel with 70 mL of diethyl ether, and the organic phase was washed successively with sodium thiosulfate solution, brine, and water. The organic phase was then dried with magnesium sulfate and filtered, and the solvents were removed in vacuo to afford 1-iodo-4-(oct-1′-ynyl)-benzene (**4**; 1.76 g, 5.64 mmol, 70%) as a pale yellow liquid. IR (cyclohexane): ν(C≡C) 2229 w cm^{-1}. ^{1}H NMR (CDCl$_3$): δ 7.58 (d, J_{HH} = 8 Hz, 2H, H$_2$), 7.09 (d, J_{HH} = 8 Hz, 2H, H$_3$), 2.36 (t, J_{HH} = 7 Hz, 2H, C$_3'$), 1.57−1.30 (m, 8H, C$_4'$−C$_7'$), 0.88 (t, J_{HH} = 7 Hz, 3H, C$_8'$). ^{13}C NMR (CDCl$_3$): δ 137.3 (C$_2$), 133.1 (C$_3$), 123.6 (C$_4$), 93.0, 92.1 (C$_1$, C$_1'$), 79.7 (C$_2'$), 31.3 (C$_3'$), 28.6 (C$_4'$), 28.5 (C$_5'$), 22.6 (C$_6'$), 19.5 (C$_7'$), 14.1 (C$_8'$). MS (EI): 312 ([M]$^+$, 99), 283 ([M − C$_2$H$_5$]$^+$, 16), 269 ([M − C$_3$H$_7$]$^+$, 47), 255 ([M − C$_4$H$_9$]$^+$, 10), 241 ([M − C$_5$H$_{11}$]$^+$, 67), 156 ([M − I − C$_2$H$_5$]$^+$, 47), 142 ([M − I − C$_3$H$_7$]$^+$, 83), 128 ([M − I − C$_4$H$_9$]$^+$, 67), 116 ([M − I − C$_5$H$_9$]$^+$, 100), 114 ([M − I − C$_5$H$_{11}$]$^+$, 66). HR-MS (EI): calcd for C$_{14}$H$_{17}$I, 312.0375; found, 312.0374.

Synthesis of Bis{4-(oct-1′-ynyl)phenyl}ethyne (5). Dichlorobis(triphenylphosphine)palladium(II) (12.7 mg, 18 μmol) and copper(I) iodide (4.2 mg, 22 μmol) were added to a solution of di(4-bromophenyl)ethyne (324 mg, 0.96 mmol), 1-octyne (0.40 mL, 0.30 mg, 2.7 mmol) and triethylamine (30 mL) at 50 °C for 6 h to afford a yellow precipitate in a brown solution. Purification by column chromatography on silica, eluting with petroleum spirit, gave a pale yellow powder identified as bis-{4-(oct-1′-ynyl)phenyl}ethyne (**5**; 132 mg, 0.34 mmol, 35%). ^{1}H NMR (CDCl$_3$): δ 7.41, 7.34 (2 × d, J_{HH} = 8 Hz, 8H, H$_2$, H$_3$), 3.48 (s, 1H, MeOH), 2.40 (t, J_{HH} = 10 Hz, 4H, H$_3'$), 1.58−1.23 (m, 16H, H$_4'$−H$_7'$), 0.88 (t, J_{HH} = 7 Hz, 6H, H$_8'$) ppm. ^{13}C NMR: δ 131.7, 131.6 (C$_2$, C$_3$), 124.3, 122.3 (C$_1$, C$_4$), 92.9 (C$_7$), 90.7 (C$_1'$), 80.5 (C$_2'$), 31.6 (C$_3'$), 28.9 (C$_4'$), 28.8 (C$_5'$), 22.8 (C$_6'$), 19.7 (C$_7'$), 14.3 (C$_8'$) ppm. MS (EI): 394 ([M]$^+$, 100), 365 ([M − Et]$^+$, 10), 323 ([M − Et − (CH$_2$)$_3$]$^+$, 32). HR-MS (EI): calcd for C$_{30}$H$_{34}$, 394.2661; found, 394.2666. Anal. Calcd for C$_{30}$H$_{34}$·$^1/_3$MeOH (394.60 + 10.68): C, 89.24; H, 8.39. Found: C, 89.67; H, 8.32.

Synthesis of 1,3,5-tris(oct-1′-ynyl)benzene (6). A solution of 1,3,5-tribromobenzene (1.02 g, 3.24 mmol), 1-octyne (2.6 mL, 17.6 mmol), dichlorobis(triphenylphosphine)palladium(II)

(104 mg, 148 μmol), and copper(I) iodide (61 mg, 320 μmol) in triethylamine (50 mL) was stirred at 65 °C for 24 h. The mixture was cooled to room temperature and the reaction mixture taken to dryness in vacuo. The residue was dissolved in petroleum spirit (3 mL) and then transferred to the top of a silica column (18 × 4 cm). The column was first eluted with petroleum spirit, increasing the polarity to petroleum spirit/dichloromethane (9/1); fractions were collected. Fractions containing the second and major band were combined, and the solvents were removed at reduced pressure (ca. 0.1 mmHg), affording a colorless oil which was identified as 1,3,5-tris(oct-1′-ynyl)benzene (**6**; 0.728 g, 1.81 mmol, 56%). A small amount of contaminant, most likely the homocoupled product of 1-octyne, namely Me(CH$_2$)$_5$C≡CC≡C(CH$_2$)$_5$Me, could not be completely removed by chromatographic techniques. The small scale of the reaction precluded efficient purification by distillation. ^{1}H NMR (CDCl$_3$): δ 7.28 (s, 3H, H$_2$), 2.35 (t, J_{HH} = 7 Hz, 6H, H$_3'$), 1.53−1.24 (m, 24H, H$_4'$−H$_7'$), 0.86 (t, J_{HH} = 7 Hz, 9H, H$_8'$). ^{13}C NMR (CDCl$_3$): δ 133.5 (C$_2$), 124.3 (C$_1$), 91.1 (C$_1'$), 79.4 (C$_2'$), 31.4 (C$_3'$), 28.7 (C$_4'$), 28.6 (C$_5'$), 22.6 (C$_6'$), 19.4 (C$_7'$), 14.1 (C$_8'$). MS (EI): 402 ([M]$^+$, 100), 387 ([M − Me]$^+$, 3), 373 ([M − C$_2$H$_5$]$^+$, 14), 359 ([M − C$_3$H$_7$]$^+$, 35), 345 ([M − C$_4$H$_9$]$^+$, 7), 333 ([M − C$_5$H$_9$]$^+$, 52), 331 ([M − C$_5$H$_{11}$]$^+$, 31). HR-MS (EI): calcd for C$_{30}$H$_{42}$, 402.3287; found, 402.3289.

Reaction of Mo$_2$Ir$_2$(CO)$_{10}$(η^5-C$_5$H$_4$Me)$_2$ (1) with 1-Iodo-4-(oct-1′-ynyl)benzene (4). 1-Iodo-4-(oct-1′-ynyl)benzene (**4**; 180 mg, 0.577 mmol) was added to a red-brown solution of **1** (233 mg, 0.230 mmol) in CH$_2$Cl$_2$ (20 mL) and the resultant mixture heated at reflux for 15 h, or until TLC and/or IR indicated the disappearance of **1**. Over the course of the reaction the color changed from red-brown to green-brown. The reaction mixture was taken to dryness on a rotary evaporator, and the residue was dissolved in a small volume (ca. 3 mL) of CH$_2$Cl$_2$ and applied to preparative TLC plates. Elution with CH$_2$Cl$_2$/petroleum spirit (1/1) gave four bands. The first band (R_f = 0.74) contained trace amounts of an unidentified black solid. The second band (R_f = 0.70) contained an unidentified orange solid (1.3 mg). IR (CH$_2$Cl$_2$): ν(CO) 2060 vs, 2020 s, 1997 m, 1832 m cm^{-1}. The third band (R_f = 0.67) contained trace amounts of an unidentified brown solid. The contents of the fourth and major band (R_f = 0.62) were crystallized from CH$_2$Cl$_2$/ethanol at 3 °C to afford dark green crystals of Mo$_2$Ir$_2${μ_4-η^2-Me(CH$_2$)$_5$C$_2$-4-C$_6$H$_4$I}(CO)$_8$(η^5-C$_5$H$_4$Me)$_2$ (**7**; 178 mg, 0.140 mmol, 61%). IR (CH$_2$Cl$_2$): ν(CO) 2066 vs, 2039 vs, 2011 m, 1994 m, 1815 s, 1767 m cm^{-1}. ^{1}H NMR (CDCl$_3$): δ 7.47 (d, J_{HH} = 9 Hz, 2H, C$_6$H$_4$), 6.80 (d, J_{HH} = 9 Hz, 2H, C$_6$H$_4$), 5.28 (s, 2H, CH$_2$Cl$_2$), 4.84−4.35 (m, 8H, C$_5$H$_4$Me), 2.76 (t, J_{HH} = 8 Hz, CH_2(CH$_2$)$_4$Me), 1.97 (s, 6H, C$_5$H$_4$Me), 1.50−1.34 (m, 8H, CH$_2$(CH_2)$_4$Me), 0.93 (t, J_{HH} = 6 Hz, 3H, (CH$_2$)$_5$Me). MS (SI): 1270 ([M]$^+$, 31), 1242 ([M − CO]$^+$, 23), 1214 ([M − 2CO]$^+$, 20), 1186 ([M − 3CO]$^+$, 43), 1158 ([M − 4CO]$^+$, 100), 1143 ([M − I]$^+$, 21), 1130 ([M − 5CO]$^+$, 55), 1115 ([M − I − CO]$^+$, 23), 1102 ([M − 6CO]$^+$, 29). Anal. Calcd for C$_{34}$H$_{31}$IIr$_2$Mo$_2$O$_8$·CH$_2$Cl$_2$ (1270.80): C, 31.01; H, 2.45. Found: C, 31.30; H, 2.35.

Synthesis of Mo$_2$Ir$_2${μ_4-η^2-Me(CH$_2$)$_5$C$_2$-4-C$_6$H$_4$C≡CSiMe$_3$}-(CO)$_8$(η^5-C$_5$H$_4$Me)$_2$ (8). To a solution of Mo$_2$Ir$_2${μ_4-η^2-Me-(CH$_2$)$_5$C$_2$-4-C$_6$H$_4$I}(CO)$_8$(η^5-C$_5$H$_4$Me)$_2$ (**7**; 145 mg, 0.114 mmol) in THF (20 mL) and triethylamine (0.5 mL) were added (trimethylsilyl)acetylene (0.25 mL, 174 mg, 1.77 mmol), dichlorobis(triphenylphosphine)palladium(II) (7 mg, 10 μmol), and copper(I) iodide (5 mg, 26 μmol), and the resultant mixture was stirred at room temperature for 4 h. The volatile materials were removed in vacuo, and the residue was dissolved in a small volume (ca. 3 mL) of CH$_2$Cl$_2$ and the solution applied to preparative TLC plates. Elution with CH$_2$Cl$_2$/petroleum spirit (2/5) gave two bands. The contents of the first and major band (R_f = 0.48) were crystallized from CH$_2$Cl$_2$/methanol at 3 °C to afford dark green crystals of Mo$_2$Ir$_2${μ_4-η^2-Me(CH$_2$)$_5$C$_2$-4-C$_6$H$_4$C≡CSiMe$_3$}(CO)$_8$(η^5-C$_5$H$_4$Me)$_2$ (**8**; 125 mg, 0.101 mmol, 88%). IR (CH$_2$Cl$_2$): ν(C≡C) 2156 w; ν(CO) 2066 vs, 2038 vs, 2010 m, 1993 m, 1814 s, 1766 m cm^{-1}. ^{1}H NMR (CDCl$_3$): δ 7.26 (d,

J_{HH} = 8 Hz, 2H, C_6H_4), 6.96 (d, J_{HH} = 8 Hz, 2H, C_6H_4), 4.82–4.33 (m, 8H, C_5H_4Me), 2.78 (t, J_{HH} = 8 Hz, 2H, $CH_2(CH_2)_4$Me), 1.95 (s, 6H, C_5H_4Me), 1.45–1.33 (m, 8H, $CH_2(CH_2)_4$Me), 0.93 (t, J_{HH} = 6 Hz, 3H, $(CH_2)_5Me$), 0.23 (s, 9H, SiMe_3). MS (SI): 1240 ([M]$^+$, 15), 1212 ([M − CO]$^+$, 9), 1184 ([M − 2CO]$^+$, 9), 1156 ([M − 3CO]$^+$, 19), 1128 ([M − 4CO]$^+$, 100), 1100 ([M − 5CO]$^+$, 55), 1072 ([M − 6CO]$^+$, 34), 1044 ([M − 7CO]$^+$, 32), 1039 ([M − C_6H_4C≡CSiMe$_3$ − CO]$^+$, 52), 1016 ([M − 8CO]$^+$, 25), 1011 ([M − C_6H_4C≡CSiMe$_3$ − 2CO]$^+$, 44). Anal. Calcd for $C_{39}H_{40}Ir_2Mo_2O_8Si$ (1241.11): C, 37.74; H, 3.25. Found: C, 37.56; H, 3.05. The second band (R_f = 0.26, green), which appeared to be in a trace amount, was not isolated.

Synthesis of Mo$_2$Ir$_2${μ_4-η^2-Me(CH$_2$)$_5$C$_2$-4-C$_6$H$_4$C≡CH}-(CO)$_8$(η^5-C$_5$H$_4$Me)$_2$ (9). A solution of Mo$_2$Ir$_2${μ_4-η^2-Me(CH$_2$)$_5$C$_2$-4-C$_6$H$_4$C≡CSiMe$_3$}(CO)$_8$(η^5-C$_5$H$_4$Me)$_2$ (**8**; 98.0 mg, 0.0789 mmol) in methanol (15 mL, not dried and distilled before use) and CH$_2$Cl$_2$ (10 mL) was deoxygenated by bubbling with nitrogen for 2 min, and then K$_2$CO$_3$ (33 mg, 0.239 mmol) was added. The resultant suspension was stirred (under nitrogen) at room temperature for 1 h. The reaction mixture was transferred to a 250 mL separating funnel, and CH$_2$Cl$_2$ (30 mL) was added. After it was washed with water (2 × 50 mL), the organic phase was dried with MgSO$_4$ and filtered and the filtrate taken to dryness on a rotary evaporator (without heating) to yield Mo$_2$Ir$_2${μ_4-η^2-Me(CH$_2$)$_5$C$_2$-4-C$_6$H$_4$C≡CH}(CO)$_8$(η^5-C$_5$H$_4$Me)$_2$ (**9**; 72.1 mg, 0.0617 mmol, 78%). IR (CH$_2$Cl$_2$): ν(C≡C) 2102 vw; ν(CO) 2066 vs, 2039 vs, 2010 m, 1993 m, 1814 s, 1767 m cm^{-1}. ^{1}H NMR (CDCl$_3$): δ 7.28 (d, J_{HH} = 8 Hz, 2H, C_6H_4), 6.99 (d, J_{HH} = 8 Hz, 2H, C_6H_4), 4.84–4.34 (m, 8H, C_5H_4Me), 3.12 (s, 1H, C≡CH), 2.78 (t, J_{HH} = 8 Hz, 2H, $CH_2(CH_2)_4$Me), 1.96 (s, 6H, C_5H_4Me), 1.45–1.33 (m, 8H, $CH_2(CH_2)_4$Me), 0.93 (t, J_{HH} = 6 Hz, 3H, $(CH_2)_5Me$). MS (SI): 1168 ([M]$^+$, 7), 1140 ([M − CO]$^+$, 9), 1112 ([M − 2CO]$^+$, 12), 1084 ([M − 3CO]$^+$, 35), 1056 ([M − 4CO]$^+$, 100), 1028 ([M − 5CO]$^+$, 55), 1000 ([M − 6CO]$^+$, 63), 971 ([M − 7CO − H]$^+$, 57), 943 ([M − 8CO − H]$^+$, 52). The instability of this complex has precluded satisfactory microanalysis.

General Procedure I for the Reaction of M$_2$Ir$_2$(CO)$_{10}$-(η^5-C$_5$H$_4$Me)$_2$ (M = Mo (1), W (2)) with Di- and Triynes. The di- or triyne was added to a red-brown solution of M$_2$Ir$_2$-(CO)$_{10}$(η^5-C$_5$H$_4$Me)$_2$ (**1, 2**) (in excess) in CH$_2$Cl$_2$ or THF (ca. 20 mL) and the resultant mixture heated at reflux until TLC and/or IR indicated no further change. Over the course of the reaction the color changed from red-brown to green-brown. The reaction mixture was taken to dryness on a rotary evaporator, and the residue was dissolved in a small volume (ca. 3 mL) of CH$_2$Cl$_2$ and the solution applied to preparative TLC plates for chromatographic separation of the products.

Reaction of Mo$_2$Ir$_2$(CO)$_{10}$(η^5-C$_5$H$_4$Me)$_2$ (1) with Bis{4-(oct-1′-ynyl)phenyl}ethyne (5). Following the general procedure I, **1** (85.0 mg, 0.084 mmol) was reacted with bis{4-(oct-1′-ynyl)phenyl}ethyne (**5**; 14.2 mg, 0.036 mmol) in CH$_2$Cl$_2$ at reflux for 24 h. Purification by preparative TLC with CH$_2$Cl$_2$/petroleum spirit (9/1) eluant gave six bands. The contents of the first band (R_f = 0.89, red-brown) were identified by solution IR as unreacted **1** (4.2 mg, 4.1 μmol). The second (R_f = 0.68, green) and third (R_f = 0.64, green) bands appeared to be in trace amounts and were not isolated. The contents of the fourth and major band (R_f = 0.54) were crystallized from CH$_2$Cl$_2$/methanol at 3 °C to afford dark green microcrystals identified as [Mo$_2$Ir$_2$(CO)$_8$(η^5-C$_5$H$_4$Me)$_2$]$_3${μ_{12}-η^6-Me(CH$_2$)$_5$C$_2$-4-C$_6$H$_4$C$_2$C$_6$H$_4$-4-C$_2$(CH$_2$)$_5$Me} (**12**; 45.0 mg, 13.8 μmol, 49% based on **1**). IR (CH$_2$Cl$_2$): ν(CO) 2067 vs, 2042 vs, 2013 sh, 1997 m, 1816 s, 1766 m cm^{-1}. UV–vis (THF): 296 sh (44.8), 376 sh (21.8), 405 (25.1), 480 sh (6.1), 634 (3.9) nm (10^3 L mol^{-1} cm^{-1}). ^{1}H NMR (CDCl$_3$): δ 7.01 (d, J_{HH} = 9 Hz, 4H, C_6H_4), 6.81 (d, J_{HH} = 9 Hz, 4H, C_6H_4), 4.97–4.38 (m, 24H, C_5H_4Me), 2.73 (t, J_{HH} = 8 Hz, 4H, $CH_2(CH_2)_5$Me), 2.00 (s, 6H, C_5H_4Me of center cluster), 1.96 (s, 12H, C_5H_4Me of outer clusters), 1.48–1.35 (m, 16H, $CH_2(CH_2)_4$Me), 0.95 (t, J_{HH} = 6 Hz, 6H, $(CH_2)_5Me$). MS (SI): 3268 ([M]$^+$, 58), 3240 ([M − CO]$^+$, 21), 3212 ([M − 2CO]$^+$, 27),

3184 ([M − 3CO]$^+$, 38), 3156 ([M − 4CO]$^+$, 29), 3128 ([M − 5CO]$^+$, 29), 3100 ([M − 6CO]$^+$, 44), 3072 ([M − 7CO]$^+$, 46), 3044 ([M − 8CO]$^+$, 40), 3016 ([M − 9CO]$^+$, 35), 2988 ([M − 10CO]$^+$, 44), 2960 ([M − 11CO]$^+$, 50), 2932 ([M − 12CO]$^+$, 52), 2904 ([M − 13CO]$^+$, 44), 2876 ([M − 14CO]$^+$, 32). Anal. Calcd for $C_{90}H_{76}Ir_6Mo_6O_{24}$ (3270.42): C, 31.47; H, 2.21. Found: C, 31.58; H, 2.30. The fifth band (R_f = 0.18) contained an unidentified green solid (1.0 mg). IR (CH$_2$Cl$_2$): ν(CO) 2067 vs, 2042 vs, 2015 m, 1997 m, 1816 s, 1766 m cm^{-1}. The sixth band (R_f = 0.12) contained an unidentified green-brown solid (1.9 mg). IR (CH$_2$Cl$_2$): ν(CO) 2067 vs, 2041 vs, 2014 m, 1997 m, 1816 s, 1766 m cm^{-1}.

Reaction of W$_2$Ir$_2$(CO)$_{10}$(η^5-C$_5$H$_4$Me)$_2$ (2) with Bis{4-(oct-1′-ynyl)phenyl}ethyne (5). Following the general procedure I, **2** (80.8 mg, 0.067 mmol) was reacted with bis{4-(oct-1′-ynyl)phenyl}ethyne (**5**; 12.1 mg, 0.031 mmol) in CH$_2$Cl$_2$ at reflux for 25 h. Purification by preparative TLC with CH$_2$Cl$_2$/petroleum spirit (9/1) eluant gave two major bands. The contents of the first band (R_f = 0.44) were crystallized from CH$_2$Cl$_2$/methanol at 3 °C to afford a dark green solid identified as [W$_2$Ir$_2$(CO)$_8$(η^5-C$_5$H$_4$Me)$_2$]$_2${μ_8-η^4-Me(CH$_2$)$_5$C$_2$-4-C$_6$H$_4$C$_2$C$_6$H$_4$-4-C≡C(CH$_2$)$_5$Me} (**13**; 4.0 mg, 1.5 μmol, 5% based on **2**). IR (CH$_2$Cl$_2$): ν(CO) 2060 vs, 2035 s, 2011 sh, 1991 m, 1812 m, 1762 m cm^{-1}. ^{1}H NMR (CDCl$_3$): δ 7.15 (d, J_{HH} = 9 Hz, 2H, C_6H_4), 7.13 (d, J_{HH} = 9 Hz, 2H, C_6H_4), 7.07 (d, J_{HH} = 9 Hz, 2H, C_6H_4), 6.85 (br d, J_{HH} = 9 Hz, 2H, C_6H_4), 4.99–4.43 (m, 16H, C_5H_4Me), 2.91 (t, J_{HH} = 9 Hz, 4H, $CH_2(CH_2)_5$Me), 2.16 (s, 12H, C_5H_4Me), 1.64–1.27 (m, 16H, $CH_2(CH_2)_4$Me), 0.98 (br t, J_{HH} = 7 Hz, 3H, $C_2(CH_2)_5Me$), 0.93 (t, J_{HH} = 7 Hz, 3H, C≡C(CH$_2$)$_5Me$). MS (FAB): 2662 ([M]$^+$, 22), 2634 ([M − CO]$^+$, 10), 2578 ([M − 3CO]$^+$, 10), 2522 ([M − 5CO]$^+$, 8), 2494 ([M − 6CO]$^+$, 18), 2466 ([M − 7CO]$^+$, 60), 2438 ([M − 8CO]$^+$, 40), 2410 ([M − 9CO]$^+$, 22), 2382 ([M − 10CO]$^+$, 14), 2354 ([M − 11CO]$^+$, 12), 2326 ([M − 12CO]$^+$, 14), 2298 ([M − 13CO]$^+$, 34), 2270 ([M − 14CO]$^+$, 40). Anal. Calcd for $C_{70}H_{62}Ir_4O_{16}W_4$ (2663.53): C, 31.57; H, 2.35. Found: C, 31.69; H, 2.50. The contents of the second and major band (R_f = 0.18) were crystallized from CH$_2$Cl$_2$/methanol at 3 °C to afford a dark green solid identified as [W$_2$Ir$_2$(CO)$_8$(η^5-C$_5$H$_4$Me)$_2$]$_3${μ_{12}-η^6-Me(CH$_2$)$_5$C$_2$-4-C$_6$H$_4$C$_2$C$_6$H$_4$-4-C$_2$(CH$_2$)$_5$Me} (**14**; 45.0 mg, 13.8 μmol, 49% based on **2**). IR (CH$_2$Cl$_2$): ν(CO) 2053 vs, 2033 s, 2013 sh, 1990 m, 1814 m, 1762 m cm^{-1}. ^{1}H NMR (CDCl$_3$): δ 7.06 (d, J_{HH} = 9 Hz, 4H, C_6H_4), 6.88 (d, J_{HH} = 9 Hz, 4H, C_6H_4), 4.98–4.41 (m, 24H, C_5H_4Me), 2.85 (br t, J_{HH} = 8 Hz, 4H, $CH_2(CH_2)_5$Me), 2.14 (s, 18H, C_5H_4Me), 1.55–1.23 (m, 16H, $CH_2(CH_2)_4$Me), 0.95 (br t, J_{HH} = 6 Hz, 6H, $(CH_2)_5Me$). MS (FAB): 3796 ([M]$^+$, 26), 3712 ([M − 3CO]$^+$, 14), 3684 ([M − 4CO]$^+$, 10), 3656 ([M − 5CO]$^+$, 18), 3628 ([M − 6CO]$^+$, 22), 3572 ([M − 8CO]$^+$, 18), 3544 ([M − 9CO]$^+$, 38), 3516 ([M − 10CO]$^+$, 70), 3488 ([M − 11CO]$^+$, 42), 3432 ([M − 13CO]$^+$, 22), 3376 ([M − 15CO]$^+$, 28), 3348 ([M − 16CO]$^+$, 38), 3320 ([M − 17CO]$^+$, 46), 3292 ([M − 18CO]$^+$, 54), 3264 ([M − 19CO]$^+$, 60), 3236 ([M − 20CO]$^+$, 72), 3180 ([M − 22CO]$^+$, 30), 3152 ([M − 23CO]$^+$, 38), 3124 ([M − 24CO]$^+$, 65). Anal. Calcd for $C_{90}H_{76}Ir_6O_{24}W_6$ (3798.00): C, 28.46; H, 2.02. Found: C, 28.44; H, 2.27.

Reaction of Mo$_2$Ir$_2$(CO)$_{10}$(η^5-C$_5$H$_4$Me)$_2$ (1) with 1,3,5-tris(oct-1′-ynyl)benzene (6). Following the general procedure I, **1** (83.2 mg, 0.082 mmol) was reacted with excess 1,3,5-tris(oct-1′-ynyl)benzene (**6**; 122 mg, 0.303 mmol) in CH$_2$Cl$_2$ at reflux for 20 h. Purification by preparative TLC with CH$_2$Cl$_2$/petroleum spirit (1/1) eluant gave eight bands. The first (R_f = 0.92, orange) and second (R_f = 0.85, orange) bands appeared to be in trace amounts and were not isolated. The contents of the third band (R_f = 0.73) afforded a dark green oil identified as Mo$_2$Ir$_2${μ_4-η^2-Me(CH$_2$)$_5$C$_2$C$_6$H$_3$-3,5-[C≡C(CH$_2$)$_5$Me]$_2$}(CO)$_8$-(η^5-C$_5$H$_4$Me)$_2$ (**15**; 17.2 mg, 0.013 mmol, 15% based on **1**). IR (CH$_2$Cl$_2$): ν(C≡C) 2229 vw; ν(CO) 2066 vs, 2039 vs, 2010 m, 1994 m, 1814 s, 1767 m cm^{-1}. ^{1}H NMR (CDCl$_3$): δ 7.07 (br t, J_{HH} = 2 Hz, 1H, C_6H_3), 6.89 (br d, J_{HH} = 2 Hz, 2H, C_6H_3), 4.81–4.29 (m, 8H, C_5H_4Me), 2.80 (t, J_{HH} = 8 Hz, 2H, C$_2$CH_2(CH$_2$)$_5$Me), 2.38 (t, J_{HH} = 7 Hz, 4H, C≡CCH_2(CH$_2$)$_5$Me),

1.97 (s, 6H, C_5H_4Me), 1.62−1.27 (m, 24H, $CH_2(CH_2)_4Me$), 0.94 (t, $J_{HH} = 6$ Hz, 3H, $C_2(CH_2)_5Me$), 0.89 (t, $J_{HH} = 7$ Hz, 6H, C≡C$(CH_2)_5Me$). MS (SI): 1360 ([M]$^+$, 27), 1332 ([M − CO]$^+$, 26), 1304 ([M − 2CO]$^+$, 35), 1276 ([M − 3CO]$^+$, 36), 1248 ([M − 4CO]$^+$, 100), 1220 ([M − 5CO]$^+$, 80), 1192 ([M − 6CO]$^+$, 55), 1164 ([M − 7CO]$^+$, 52), 1136 ([M − 8CO]$^+$, 50). The contents of the fourth band ($R_f = 0.60$) afforded a dark green oil identified as $Mo_2Ir_2\{\mu_4\text{-}\eta^2\text{-}Me(CH_2)_5C_2C≡C(CH_2)_5Me\}(CO)_8(\eta^5\text{-}C_5H_4Me)_2$ (**17**; 2.1 mg, 1.8 μmol, 2% based on **1**). This adduct most likely results from reaction of **1** with a contaminant that could not be completely removed during the synthesis of the triyne **6** (see above). IR (CH$_2$Cl$_2$): ν(C≡C) 2224 vw; ν(CO) 2065 vs, 2038 vs, 2013 m, 1993 m, 1814 s, 1766 m cm^{-1}. ^{1}H NMR (CDCl$_3$): 4.93−4.62 (m, 8H, C_5H_4Me), 2.89 (br s, 2H, $C_2CH_2(CH_2)_5$-Me), 2.28 (t, $J_{HH} = 6$ Hz, 2H, C≡C$CH_2(CH_2)_5Me$), 2.06 (s, 6H, C_5H_4Me), 1.46−1.17 (m, 16H, $CH_2(CH_2)_4Me$), 0.93−0.83 (m, 6H, $(CH_2)_5Me$). MS (SI): 1176 ([M]$^+$, 62), 1148 ([M − CO]$^+$, 50), 1120 ([M − 2CO]$^+$, 74), 1092 ([M − 3CO]$^+$, 56), 1064 ([M − 4CO]$^+$, 94), 1036 ([M − 5CO]$^+$, 56), 1008 ([M − 6CO]$^+$, 64), 980 ([M − 7CO]$^+$, 71), 952 ([M − 8CO]$^+$, 55). The fifth ($R_f = 0.47$, brown) and sixth ($R_f = 0.44$, brown) bands appeared to be in trace amounts and were not isolated. The seventh band ($R_f = 0.36$) contained an unidentified green solid (3.8 mg). IR (CH$_2$Cl$_2$): ν(CO) 2068 vs, 2039 vs, 2011 m, 1991 s, 1966 sh, 1816 s, 1770 m cm^{-1}. The contents of the eighth band ($R_f = 0.33$) afforded a dark green oily solid identified as $[Mo_2Ir_2(CO)_8(\eta^5\text{-}C_5H_4Me)_2]_2\{\mu_8\text{-}\eta^4\text{-}[Me(CH_2)_5C_2]_2\text{-}1,3\text{-}C_6H_3\text{-}5\text{-}C≡C(CH_2)_5\text{-}Me\}$ (**16**; 25.3 mg, 0.011 mmol, 27% based on **1**). IR (CH$_2$Cl$_2$): ν(C≡C) 2228 vw; ν(CO) 2069 vs, 2040 vs, 2009 m, 1991 s, 1818 s, 1770 m cm^{-1}. ^{1}H NMR (CDCl$_3$): δ 6.80 (br s, 2H, C$_6$H$_3$), 6.21 (br s, 1H, C$_6$H$_3$), 4.95−4.24 (br m, 16H, C_5H_4Me), 2.92 (vbr s, 4H, $C_2CH_2(CH_2)_5Me$), 2.38 (t, $J_{HH} = 8$ Hz, 2H, C≡CCH_2-$(CH_2)_5Me$), 2.05 (s, 12H, C_5H_4Me), 1.61−1.20 (m, 24H, CH_2-$(CH_2)_4Me$), 0.94 (t, $J_{HH} = 7$ Hz, 6H, C$_2(CH_2)_5Me$), 0.86 (t, $J_{HH} = 8$ Hz, 3H, C≡C$(CH_2)_5Me$). MS (SI): 2206 ([M − 4CO]$^+$, 20), 2178 ([M − 5CO]$^+$, 24), 2150 ([M − 6CO]$^+$, 20), 2122 ([M − 7CO]$^+$, 22), 2094 ([M − 8CO]$^+$, 25), 2066 ([M − 9CO]$^+$, 34), 2038 ([M − 10CO]$^+$, 25), 2010 ([M − 11CO]$^+$, 52), 1982 ([M − 12CO]$^+$, 47), 1954 ([M − 13CO]$^+$, 55), 1926 ([M − 14CO]$^+$, 50), 1898 ([M − 15CO]$^+$, 41), 1870 ([M − 16CO]$^+$, 63).

Reaction of $Mo_2Ir_2(CO)_{10}(\eta^5\text{-}C_5H_4Me)_2$ (1) with $[Mo_2Ir_2\text{-}(CO)_8(\eta^5\text{-}C_5H_4Me)_2]_2\{\mu_8\text{-}\eta^4\text{-}[Me(CH_2)_5C_2]_2\text{-}1,3\text{-}C_6H_3\text{-}5\text{-}C≡C\text{-}(CH_2)_5Me\}$ (16). A mixture of $Mo_2Ir_2(CO)_{10}(\eta^5\text{-}C_5H_4Me)_2$ (**1**; 24.1 mg, 23.8 μmol) and $[Mo_2Ir_2(CO)_8(\eta^5\text{-}C_5H_4Me)_2]_2\{\mu_8\text{-}\eta^4\text{-}[Me\text{-}(CH_2)_5C_2]_2\text{-}1,3\text{-}C_6H_3\text{-}5\text{-}C≡C(CH_2)_5Me\}$ (**16**; 25.0 mg, 10.8 μmol) in CH$_2$Cl$_2$ (10 mL) was heated at reflux for 4 h. The brown solution was cooled and taken to dryness, and the resulting residue was applied to preparative TLC plates. Elution with CH$_2$Cl$_2$/petroleum spirit (4/1) gave two bands. The contents of the first band ($R_f = 0.92$, red-brown) were identified by solution IR as unreacted **1** (20.1 mg, 19.8 μmol). The contents of the second band ($R_f = 0.68$) afforded a dark green-brown solid (23.1 mg) which was studied by ^{1}H NMR, IR, and SI mass spectrometry. Attempts to recrystallize this substance (possibly a mixture) resulted in decomposition. IR (CH$_2$Cl$_2$): ν(CO) 2069 vs, 2040 s, 2010 sh, 1990 s, 1951 w, 1886 w, 1819 s, 1771 m cm^{-1}. ^{1}H NMR (CDCl$_3$): complex series of resonances in the range δ 7.10−1.80. MS (SI): no distinct fragment peaks.

Reaction of $Mo_2Ir_2\{\mu_4\text{-}\eta^2\text{-}Me(CH_2)_5C_2\text{-}4\text{-}C_6H_4I\}(CO)_8(\eta^5\text{-}C_5H_4Me)_2$ (7) and $Mo_2Ir_2\{\mu_4\text{-}\eta^2\text{-}Me(CH_2)_5C_2\text{-}4\text{-}C_6H_4C≡CH\}\text{-}(CO)_8(\eta^5\text{-}C_5H_4Me)_2$ (9). To a solution of $Mo_2Ir_2\{\mu_4\text{-}\eta^2\text{-}Me\text{-}(CH_2)_5C_2\text{-}4\text{-}C_6H_4I\}(CO)_8(\eta^5\text{-}C_5H_4Me)_2$ (**7**; 66 mg, 0.052 mmol) and $Mo_2Ir_2\{\mu_4\text{-}\eta^2\text{-}Me(CH_2)_5C_2\text{-}4\text{-}C_6H_4C≡CH\}(CO)_8(\eta^5\text{-}C_5H_4Me)_2$ (**9**; 61 mg, 0.052 mmol) in THF (5 mL) and triethylamine (0.2 mL) were added dichlorobis(triphenylphosphine)palladium(II) (1.0 mg, 1.4 μmol) and copper(I) iodide (1.6 mg, 8.4 μmol), and the resultant mixture was stirred at room temperature for 40 h. The reaction mixture was taken to dryness, and the residue was dissolved in a small volume (ca. 3 mL) of CH$_2$Cl$_2$ and the solution applied to preparative TLC plates. Elution with CH$_2$Cl$_2$/petroleum spirit (1/1) gave three bands. The contents

of the first band ($R_f = 0.62$) were identified by solution IR and ^{1}H NMR as unreacted $Mo_2Ir_2\{\mu_4\text{-}\eta^2\text{-}Me(CH_2)_5C_2\text{-}4\text{-}C_6H_4I\}(CO)_8$-$(\eta^5\text{-}C_5H_4Me)_2$ (**7**; 29.1 mg, 0.023 mmol). The second ($R_f = 0.43$) and third bands ($R_f = 0.40$) were collected together and rechromatographed by TLC, developing a further two times with CH$_2$Cl$_2$/petroleum spirit (3/2) as eluent, to give two separate bands. The contents of the first band ($R_f = 0.45$) were crystallized from CH$_2$Cl$_2$/methanol at 3 °C to afford dark green crystals of $[Mo_2Ir_2(CO)_8(\eta^5\text{-}C_5H_4Me)_2]_2\{\mu_8\text{-}\eta^4\text{-}Me(CH_2)_5C_2\text{-}4\text{-}C_6H_4C≡CC≡CC_6H_4\text{-}4\text{-}C_2(CH_2)_5Me\}$ (**19**; 9.3 mg, 4.0 μmol, 8%). A crystal grown by this method was selected for a single-crystal X-ray structural study. IR (CH$_2$Cl$_2$): ν(CO) 2066 vs, 2039 vs, 2010 w, 1994 m, 1815 s, 1768 m cm^{-1}. ^{1}H NMR (CDCl$_3$): δ 7.31 (d, $J_{HH} = 8$ Hz, 4H, C$_6$H$_4$), 7.01 (d, $J_{HH} = 8$ Hz, 4H, C$_6$H$_4$), 4.84−4.35 (m, 16H, C_5H_4Me), 2.77 (t, $J_{HH} = 8$ Hz, 4H, $CH_2(CH_2)_4Me$), 1.96 (s, 12H, C_5H_4Me), 1.45−1.32 (m, 16H, CH_2-$(CH_2)_4Me$), 0.93 (t, $J_{HH} = 6$ Hz, 6H, $(CH_2)_5Me$). MS (SI): 2334 ([M]$^+$, 19), 2306 ([M − CO]$^+$, 15), 2278 ([M − 2CO]$^+$, 11), 2250 ([M − 3CO]$^+$, 44), 2222 ([M − 4CO]$^+$, 30), 2194 ([M − 5CO]$^+$, 23), 2166 ([M − 6CO]$^+$, 44), 2138 ([M − 7CO]$^+$, 60), 2110 ([M − 8CO]$^+$, 73), 2082 ([M − 9CO]$^+$, 100), 2054 ([M − 10CO]$^+$, 54). Anal. Calcd for C$_{72}$H$_{62}$Ir$_4$Mo$_4$O$_{16}$ (2335.84): C, 37.02; H, 2.68. Found: C, 36.82; H, 2.81. The contents of the second and major band ($R_f = 0.42$) were crystallized from CH$_2$Cl$_2$/methanol at 3 °C to afford dark green crystals of $[Mo_2Ir_2(CO)_8(\eta^5\text{-}C_5H_4Me)_2]_2\{\mu_8\text{-}\eta^4\text{-}Me(CH_2)_5C_2\text{-}4\text{-}C_6H_4C≡CC_6H_4\text{-}4\text{-}C_2(CH_2)_5\text{-}Me\}$ (**18**; 28.5 mg, 12.3 μmol, 24%). IR (CH$_2$Cl$_2$): ν(CO) 2066 vs, 2039 vs, 2010 w, 1994 m, 1815 s, 1768 m cm^{-1}. UV−vis (THF): 289 sh (41.4), 321 sh (30.8), 388 (28.3), 408 sh (26.9), 631 (2.9) nm (10^3 L mol^{-1} cm^{-1}). ^{1}H NMR (CDCl$_3$): δ 7.30 (d, $J_{HH} = 8$ Hz, 4H, C$_6$H$_4$), 7.03 (d, $J_{HH} = 8$ Hz, 4H, C$_6$H$_4$), 4.85−4.36 (m, 16H, C_5H_4Me), 2.79 (t, $J_{HH} = 8$ Hz, 4H, $CH_2(CH_2)_4$-Me), 1.96 (s, 12H, C_5H_4Me), 1.46−1.32 (m, 16H, $CH_2(CH_2)_4Me$), 0.94 (t, $J_{HH} = 6$ Hz, 6H, $(CH_2)_5Me$). MS (SI): 2310 ([M]$^+$, 34), 2282 ([M − CO]$^+$, 5), 2254 ([M − 2CO]$^+$, 13), 2226 ([M − 3CO]$^+$, 30), 2198 ([M − 4CO]$^+$, 5), 2170 ([M − 5CO]$^+$, 21), 2142 ([M − 6CO]$^+$, 34), 2114 ([M − 7CO]$^+$, 71), 2086 ([M − 8CO]$^+$, 88), 2058 ([M − 9CO]$^+$, 54), 2030 ([M − 10CO]$^+$, 48). Anal. Calcd for C$_{70}$H$_{62}$Ir$_4$Mo$_4$O$_{16}$ (2311.81): C, 36.37; H, 2.70. Found: C, 36.54; H, 2.90.

Electrochemical Studies. The cyclic voltammograms were recorded using a MacLab 400 interface and MacLab potentiostat from ADInstruments. The supporting electrolyte was 0.25 M (NBu$^n_4$)PF$_6$ in distilled, deoxygenated CH$_2$Cl$_2$. Solutions containing on the order of millimolar concentrations of complex were maintained under argon. Measurements were carried out using a platinum-disk working electrode, a platinum auxiliary electrode, and an Ag/AgCl reference electrode, using the ferrocene/ferrocenium redox couple as an internal reference (0.56 V).

X-ray Crystallographic Study. A single crystal was mounted on the side of a fine glass capillary using Paratone oil, and data were collected at 200 K on a Nonius KappaCCD diffractometer using graphite-monochromated Mo Kα radiation ($\lambda = 0.710\,69$ Å). The unit cell refinement, data reduction,[40] and absorption correction[41] were implemented from within maXus.[42] The structure was solved by direct[43] methods and expanded using difference Fourier techniques[44] from within the teXsan software package.[45] Non-hydrogen atoms were refined anisotropically; hydrogen atoms were included

(40) Otwinowski, Z.; Minor, W. In *Methods in Enzymology*; Carter, C. W., Jr., Sweet, R. M., Eds.; Academic Press: New York, 1997; Vol. 276, p 307.

(41) Coppens, P. In *Crystallographic Computing*; Ahmed, F. R., Hall, S. R., Huber, C. P., Eds.; Munksgaard: Copenhagen, 1970; p 255.

(42) Mackay, S.; Gilmore, C. J.; Edwards, C.; Stewart, N.; Shankland, K. maXus: Computer Program for the Solution and Refinement of Crystal Structures; Nonius (The Netherlands), MacScience (Japan), and The University of Glasgow (U.K.), 1999.

(43) Altomare, A.; Cascarano, M.; Giacovazzo, C.; Guagliardi, A.; Burla, M. C.; Polidori, G.; Camalli, M. *J. Appl. Crystallogr.* **1994**, *27*, 425.

Table 1. Crystal Data for 19

formula	$C_{72}H_{62}Ir_4Mo_4O_{16}$
fw	2335.91
cryst size (mm)	$0.15 \times 0.15 \times 0.14$
color, habit	dark green, block
cryst syst	monoclinic
space group	$P2_1/c$ (No. 14)
a (Å)	9.8756(2)
b (Å)	18.4541(3)
c (Å)	19.2548(3)
β (deg)	101.8589(8)
V (Å^3)	3434.20(9)
Z	2
D_{calcd} (g cm^{-3})	2.26
μ (mm^{-1})	8.511
θ_{max} (deg)	25.05
index ranges	$-11 \leq h \leq 11$
	$-21 \leq k \leq 21$
	$-22 \leq l \leq 22$
N_{measd}	54 003
N_{unique} (R_{int})	6061 (0.0874)
N_{obs} ($I > 3\sigma(I)$)	3930
abs corr	integration
T_{min}, T_{max}	0.30, 0.50
N_{param}	418
R ($I > 3\sigma(I)$)^a	0.056
R_w ($I > 3\sigma(I)$)^b	0.083
GOF	1.76
largest diff peak, hole (e Å^{-3})	3.43, -2.31

^{a} $R = \Sigma||F_o| - |F_c||/\Sigma|F_o|$. ^{b} $R_w = [(\Sigma w(|F_o| - |F_c|)^2/\Sigma wF_o^2]^{1/2}$, $w = \sigma_c^2(F_o) + 0.00040F_o^2]^{-1}$.

in idealized positions which were frequently recalculated. The final cycle of full-matrix least-squares refinement on F was based on 3930 reflections and 418 parameters and converged to $R = 0.056$ and $R_w = 0.083$. The data collection and structural refinement details are summarized in Table 1, and selected bond lengths and angles are given in Table 2. A labeled molecular structure is shown in Figure 2. The molecule lies on an inversion center, and the symmetry-expanded diagram is shown.

Theoretical Methods. Approximate density functional theory calculations were performed on Linux-based Pentium III 600 MHz computers using the Amsterdam Density Functional (ADF) program, version ADF 2000.02,[46] developed by Baerends et al.[47−51] Calculations on $Mo_2Ir_2(\mu_4-\eta^2-MeC_2Ph)$-$(CO)_n(\eta^5-C_5H_5)_2$ ($n = 7, 8$) structures, in various charge states, were performed in C_s symmetry unless stated otherwise. Electrons in orbitals up to and including 1s {C, O}, 4p {Mo}, and 4f (but excluding 5s and 5p) {Ir} were treated in accordance with the frozen-core approximation. Geometry optimizations were attempted for the +1, 0, −1, and −2 charge states, using the local density approximation (LDA) to the exchange potential[52] and the correlation potential of Vosko,

(44) Beurskens, P. T.; Admiraal, G.; Beurskens, G.; Bosman, W. P.; de Gelder, R.; Israel, R.; Smits, J. M. M. The DIRDIF-94 Program System; Technical Report of the Crystallography Laboratory; University of Nijmegen, Nijmegen, The Netherlands, 1994.
(45) teXsan: Single-Crystal Structure Analysis Software, Version 1.8; Molecular Structure Corp., The Woodlands, TX 77381, 1997.
(46) Baerends, E. J.; Bérces, A.; Bo, C.; Boerrigter, P. M.; Cavallo, L.; Deng, L.; Dickson, R. M.; Ellis, D. E.; Fan, L.; Fischer, T. H.; Fonseca Guerra, C.; van Gisbergen, S. J. A.; Groeneveld, J. A.; Gritsenko, O. V.; Harris, F. E.; van den Hoek, P.; Jacobsen, H.; van Kessel, G.; Kootstra, F.; van Lenthe, E.; Osinga, V. P.; Philipsen, P. H. T.; Post, D.; Pye, C.; Ravenek, W.; Ros, P.; Schipper, P. R. T.; Schreckenbach, G.; Snijders, J. G.; Sola, M.; Swerhone, D.; te Velde, G.; Vernooijs, P.; Versluis, L.; Visser, O.; van Wezenbeek, E.; Wiesenekker, G.; Wolff, S. K.; Woo, T. K.; Ziegler, T. ADF, 2000.01, 2000.
(47) Baerends, E. J.; Ellis, D. E.; Ros, P. *Chem. Phys.* **1973**, *2*, 42.
(48) Baerends, E. J.; Ros, P. *Chem. Phys.* **1973**, *2*, 52.
(49) Versluis, L.; Ziegler, T. *J. Chem. Phys.* **1988**, *88*, 322.
(50) te Velde, G.; Baerends, E. J. *J. Comput. Chem.* **1992**, *99*, 84.
(51) Fonseca Guerra, C.; Snijders, J. G.; te Velde, G.; Baerends, E. J. *Theor. Chem. Acta* **1998**, *99*, 391.
(52) Ziegler, T. *Chem. Rev.* **1991**, *91*, 1.

Table 2. Selected Bond Lengths (Å) and Angles (deg) for [Mo$_2$Ir$_2(\mu$-CO)$_4$(CO)$_4(\eta^5$-C$_5$H$_4$Me)$_2$]$_2\{\mu_8$-η^4-Me(CH$_2$)$_5$C$_2$-4-C$_6$H$_4$C≡CC≡CC$_6$H$_4$-4-C$_2$(CH$_2$)$_5$Me$\}$ (19)

Ir1−Ir2	2.687(1)	Mo1−C6	2.00(2)
Ir1−Mo1	2.837(2)	Mo2−C7	2.06(2)
Ir1−Mo2	2.807(2)	Mo2−C8	1.95(2)
Ir2−Mo1	2.789(2)	C1−O1	1.05(2)
Ir2−Mo2	2.811(2)	C2−O2	1.13(2)
Ir1−C27	2.09(2)	C3−O3	1.12(2)
Ir2−C28	2.12(2)	C4−O4	1.15(2)
Mo1−C27	2.41(2)	C5−O5	1.14(2)
Mo1−C28	2.35(1)	C6−O6	1.18(2)
Mo2−C27	2.31(2)	C7−O7	1.11(2)
Mo2−C28	2.30(2)	C8−O8	1.15(2)
Mo1−Cp†^{a}	1.990	C27−C28	1.43(2)
Mo2−Cp†	2.009	C28−C29	1.53(2)
Ir1−C1	2.01(2)	C29−C30	1.37(2)
Ir1−C2	1.93(2)	C29−C34	1.40(2)
Ir1−C5	2.39(2)	C30−C31	1.36(2)
Ir1−C7	2.39(2)	C31−C32	1.39(2)
Ir2−C3	1.85(2)	C32−C33	1.38(2)
Ir2−C4	1.91(2)	C32−C35	1.42(2)
Ir2−C6	2.31(2)	C33−C34	1.43(2)
Ir2−C8	2.31(2)	C35−C36	1.19(2)
Mo1−C5	2.05(2)	C36−C36*	1.40(3)
Ir2−Ir1−Mo1	60.59(4)	Ir1−C2−O2	176(3)
Ir2−Ir1−Mo2	61.51(4)	Ir1−C5−O5	125(2)
Mo1−Ir1−Mo2	96.80(5)	Ir1−C7−O7	124(2)
Ir1−Ir2−Mo1	62.37(4)	Ir2−C3−O3	176(2)
Ir1−Ir2−Mo2	61.35(4)	Ir2−C4−O4	179(2)
Mo1−Ir2−Mo2	97.81(5)	Ir2−C6−O6	127(2)
Ir1−Mo1−Ir2	57.05(4)	Ir2−C8−O8	153(2)
Ir1−Mo2−Ir2	57.15(3)	Mo1−C5−O5	156(2)
Ir1−C27−Mo1	77.9(5)	Mo1−C6−O6	152(2)
Ir1−C27−Mo2	79.2(5)	Mo2−C7−O7	158(2)
Ir1−C27−C28	107(1)	Mo2−C8−O8	153(2)
Ir2−C28−Mo1	77.0(5)	C27−C28−C29	125(1)
Ir2−C28−Mo2	78.9(5)	C32−C35−C36	176(2)
Ir2−C28−C27	108(1)	C35−C36−C36*	177(2)
Ir1−C1−O1	169(3)		

^{a} Cp† = centroid of (η^5−C$_5$H$_4$Me) ring.

Wilk, and Nusair,[53] with a double-ζ quality Slater type orbital (type II) basis set for each atom. Calculations for the neutral and dianionic species were spin-restricted, while those for the radical cation and anion were unrestricted.

Nonlocal and relativistic corrections to the local density approximation were effected through single-point calculations on the LDA/type II optimized geometries, employing the B-LYP nonlocal exchange and correlation functionals and the ZORA scalar relativistic correction[54] in conjunction with triple-ζ (type IV) basis sets for each atom. We have previously found[33] that such an approach yields relative energies of different isomers and different charge states, which approximate closely to those obtained from more computationally intensive geometry optimizations, including ZORA corrections and type IV basis sets. The combination of LDA geometries and nonlocally corrected single-point total energies has also been found to reliably characterize several other aspects of carbonyl-ligated iridium-containing clusters, particularly with regard to the interchange between bridging and terminal carbonyl ligands.[55]

Results and Discussion

Synthesis of Organic π-Delocalized Frameworks. The π-delocalized frameworks chosen to link the group 6−iridium clusters have been built up using the cross-coupling of an aryl halide with a terminal alkyne in the

(53) Vosko, S. H.; Wilk, L.; Nusair, M. *Can. J. Phys.* **1980**, *58*, 1200.
(54) van Lenthe, E.; Baerends, E. J.; Snijders, J. G. *J. Chem. Phys.* **1993**, *99*, 4597.
(55) Besançon, K.; Laurenczy, G.; Lumini, T.; Roulet, R.; Bruyndonckx, R. *Inorg. Chem.* **1998**, *37*, 5634.
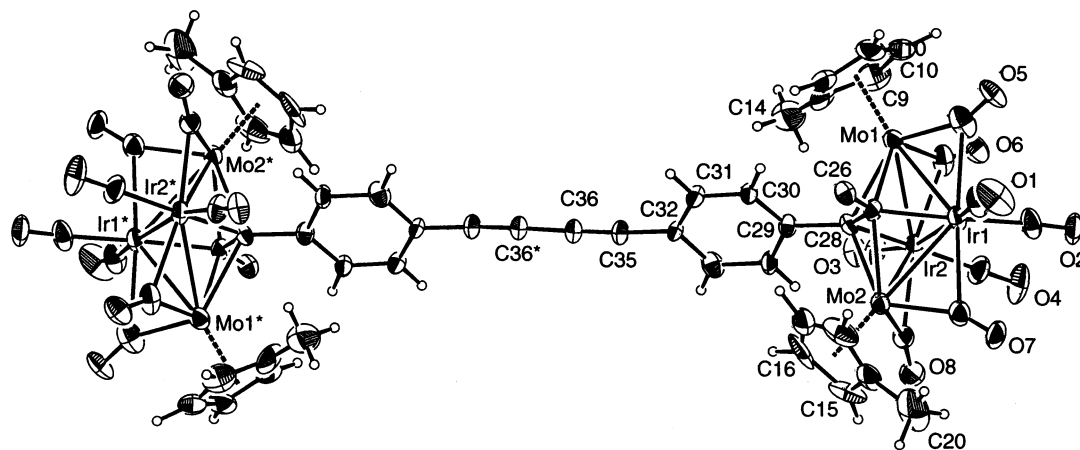
Figure 2. Molecular structure and atomic numbering scheme for **19**. Displacement ellipsoids are shown at the 30% probability level; hydrogens have an arbitrary radius.

presence of palladium(II) and copper(I) iodide catalysts (Sonogashira coupling).[56,57] The synthetic procedures are summarized in Scheme 1, all new compounds being characterized by IR and ^{1}H and ^{13}C NMR spectroscopy, EI mass spectrometry, and satisfactory microanalysis (solids) or high-resolution EI mass spectrometry (oils).

The reaction of 1-octyne with 4-bromo-1-iodobenzene in the presence of dichlorobis(triphenylphosphine)-palladium(II) and copper(I) iodide catalysts gave 1-bromo-4-(oct-1′-ynyl)benzene (**3**). The addition of 2 equiv of *tert*-butyllithium to **3** at −77 °C generated an organolithium species which, when reacted in situ with iodine, gave the transhalogenated product 1-iodo-4-(oct-1′-ynyl)ben-zene (**4**). The linear triyne bis{4-(oct-1′-ynyl)phenyl}-ethyne (**5**) has been prepared similarly, using palladium-catalyzed Sonogashira coupling of 1-octyne with bis(4-bromophenyl)ethyne. The branched triyne 1,3,5-tris(oct-1′-ynyl)benzene (**6**) was also synthesized using Sono-gashira protocols. A small amount of contaminant, most likely the homocoupled product of 1-octyne, namely Me(CH$_2$)$_5$C≡CC≡C(CH$_2$)$_5$Me, could not be completely removed from **6** by chromatographic techniques; the small scale of the reaction precluded efficient purifica-tion by distillation.

Reactions of Mo$_2$Ir$_2$(CO)$_{10}$(η^5-C$_5$H$_4$Me)$_2$ (1) with Monoynes and Syntheses of Other Monocluster Alkyne-Derived Adducts. Heating the methylcyclo-pentadienyl cluster Mo$_2$Ir$_2$(CO)$_{10}$(η^5-C$_5$H$_4$Me)$_2$ (**1**) in refluxing dichloromethane with 1-iodo-4-(oct-1′-ynyl)-benzene (**4**) afforded dark green crystals of Mo$_2$Ir$_2$(μ_4-η^2-Me(CH$_2$)$_5$C$_2$-4-C$_6$H$_4$I}(μ-CO)$_4$(CO)$_4$(η^5-C$_5$H$_4$Me)$_2$ (**7**), following chromatographic workup and crystallization, in good yield (Scheme 2). This cluster is a functionalized monoyne cluster adduct for which coupling chemistry at the iodo substituent provides one route to linked cluster compounds. Thus, palladium-catalyzed coupling of (trimethylsilyl)acetylene with **7** proceeded under mild conditions to afford the (trimethylsilyl)ethynylated de-rivative Mo$_2$Ir$_2${μ_4-η^2-Me(CH$_2$)$_5$C$_2$C$_6$H$_4$-4-C≡CSiMe$_3$}-(CO)$_8$(η^5-C$_5$H$_4$Me)$_2$ (**8**) in excellent yield following TLC and crystallization (Scheme 2). Deprotection of the (trimethylsilyl)ethynyl group of **8** was effected by reac-
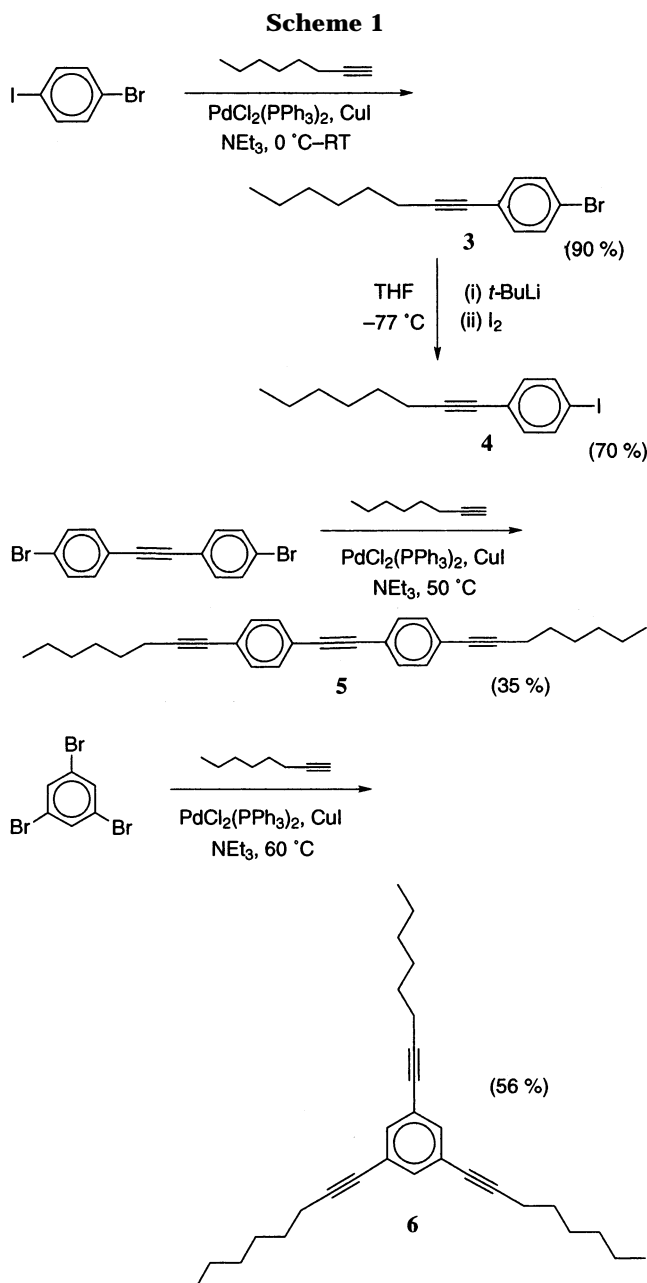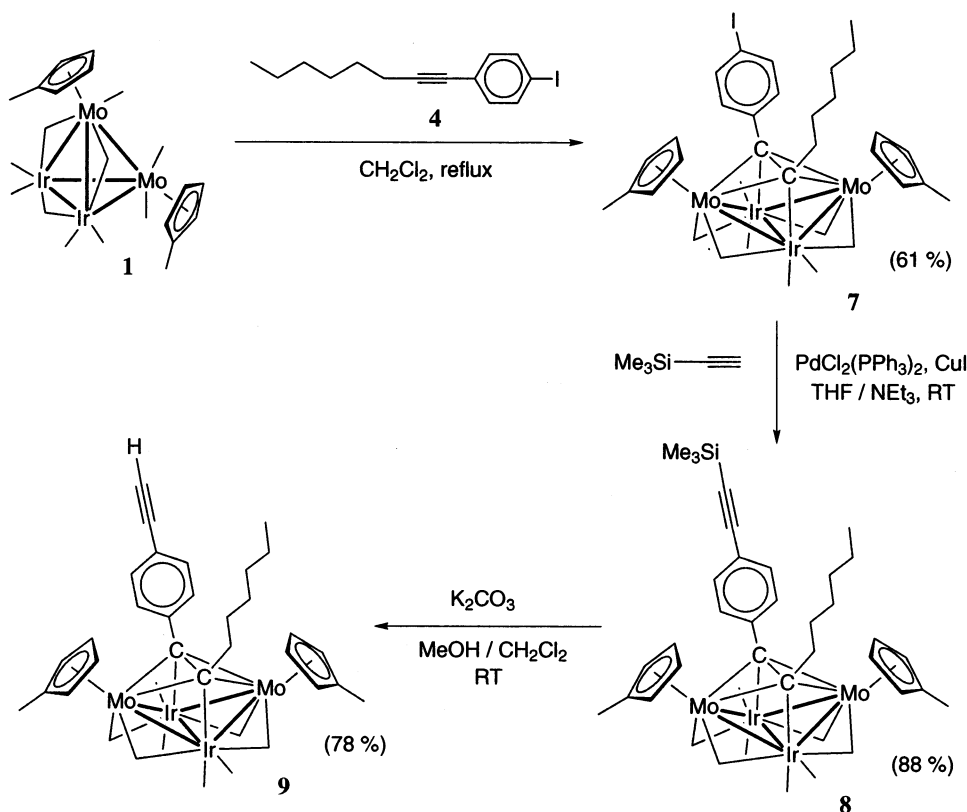
(56) Takahashi, S.; Kuroyama, Y.; Sonogashira, K.; Hagihara, N. *Synthesis* **1980**, 627.
(57) Austin, W. B.; Bilow, N.; Kelleghan, W. J.; Lau, K. S. Y. *J. Org. Chem.* **1981**, *46*, 2280.

Scheme 1

3 (90 %)

4 (70 %)

5 (35 %)

6 (56 %)

tion with potassium carbonate at room temperature in a methanol/dichloromethane mixture to afford Mo$_2$Ir$_2$-

Scheme 2

$\{\mu_4\text{-}\eta^2\text{-Me(CH}_2)_5\text{C}_2\text{C}_6\text{H}_4\text{-4-C}\equiv\text{CH}\}(\text{CO})_8(\eta^5\text{-C}_5\text{H}_4\text{Me})_2$ (**9**) as a green powder. The synthesis of **9** by this procedure is somewhat long-winded, but this product would not be accessible by direct reaction of the cluster Mo_2Ir_2-$(\text{CO})_{10}(\eta^5\text{-C}_5\text{H}_4\text{Me})_2$ (**1**) with the appropriate diyne, previous studies having shown that tetrahedral dimolybdenum–diiridium clusters such as **1** react preferentially at a terminal alkyne rather than an internal alkyne group.[58] The thermal sensitivity of the terminal alkyne group has rendered crystallization of this product unsuccessful to date. The products have been characterized by IR, ^{1}H NMR, SI mass spectrometry, and, in the case of **7** and **8**, satisfactory microanalyses. The solution IR spectra of **7**–**9** exhibit a distinctive ν(CO) pattern: four bands in the terminal carbonyl region 2066–1993 cm^{-1} and two in the bridging carbonyl region 1815–1766 cm^{-1}, accompanied by weak ν(C≡C) bands at 2156 cm^{-1} (**8**) and ca. 2100 cm^{-1} (**9**). The ^{1}H NMR spectra contain resonances arising from the phenylene units, cyclopentadienyl groups, and alkyne residue, accompanied by a signal at δ 0.23 (**8**) corresponding to the trimethylsilyl group and at δ 3.12 (**9**) corresponding to the terminal proton. The SIMS spectra contain peaks corresponding to the molecular ion and successive loss of carbonyl ligands.

Syntheses of Di- and Tricluster Adducts Linked through π-Delocalized Frameworks. We have previously demonstrated the facile formation of the linked dicluster complexes $[\text{M}_2\text{Ir}_2(\text{CO})_8(\eta^5\text{-C}_5\text{H}_4\text{Me})_2]_2\{\mu_8\text{-}\eta^4\text{-}$ $\text{Me(CH}_2)_5\text{C}_2\text{C}_6\text{H}_4\text{-4-C}_2(\text{CH}_2)_5\text{Me}\}$ (M = Mo (**10**), W (**11**)) by reaction of an excess of the tetrahedral clusters **1** and **2** with 1,4-bis(oct-1′-ynyl)benzene.[34] Similar reac-
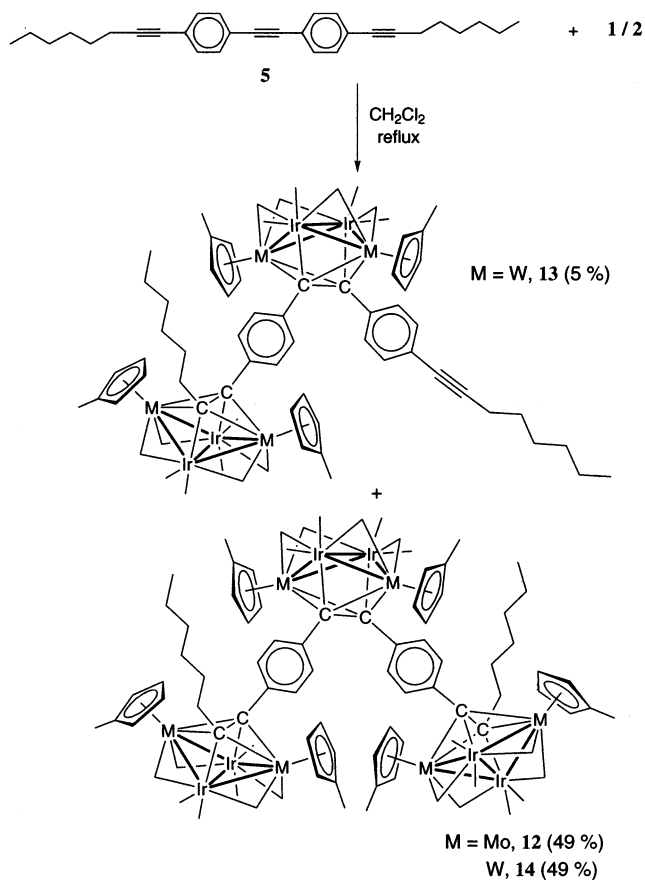
tions of an excess of $\text{M}_2\text{Ir}_2(\text{CO})_{10}(\eta^5\text{-C}_5\text{H}_4\text{Me})_2$ (**1**, **2**) with bis{4-(oct-1′-ynyl)phenyl}ethyne (**5**) in refluxing dichloromethane afforded the linked-cluster adducts $[\text{M}_2\text{Ir}_2\text{-}$ $(\text{CO})_8(\eta^5\text{-C}_5\text{H}_4\text{Me})_2]_3\{\mu_{12}\text{-}\eta^6\text{-Me(CH}_2)_5\text{C}_2\text{-4-C}_6\text{H}_4\text{C}_2\text{C}_6\text{H}_4\text{-}$ $4\text{-C}_2(\text{CH}_2)_5\text{Me}\}$ (M = Mo (**12**); W (**14**)) and $[\text{W}_2\text{Ir}_2(\text{CO})_8\text{-}$ $(\eta^5\text{-C}_5\text{H}_4\text{Me})_2]_2\{\mu_8\text{-}\eta^4\text{-Me(CH}_2)_5\text{C}_2\text{-4-C}_6\text{H}_4\text{C}_2\text{C}_6\text{H}_4\text{-4-C}\equiv\text{C-}$ $(\text{CH}_2)_5\text{Me}\}$ (**13**) (Scheme 3).

Products **12** and **14**, which result from coordination of cluster units at each of the three C≡C sites on the triyne, and **13**, which results from coordination of cluster units at two adjacent C≡C sites, were characterized by a combination of IR, ^{1}H NMR, and UV−vis spectroscopy, SI mass spectrometry, and satisfactory microanalyses. The solution infrared spectra of **12**−**14** exhibit the characteristic four-terminal-bands, two-bridging-bands ν(CO) pattern for the $\text{M}_2\text{Ir}_2\text{C}_2$ cluster type, and the SIMS spectra contain molecular ions and envelopes corresponding to successive CO loss. The ^{1}H NMR spectra of **12** and **14** contain characteristic methylcyclopentadienyl, phenylene, and hexyl group resonances in the appropriate ratios, confirming their identities as tricluster adducts, while the ^{1}H NMR spectrum of **13** contains these resonances in ratios confirming **13** as a dicluster adduct; the number of signals in the aromatic region for the latter is only consistent with the (lower symmetry) cluster coordination at adjacent C≡C sites.
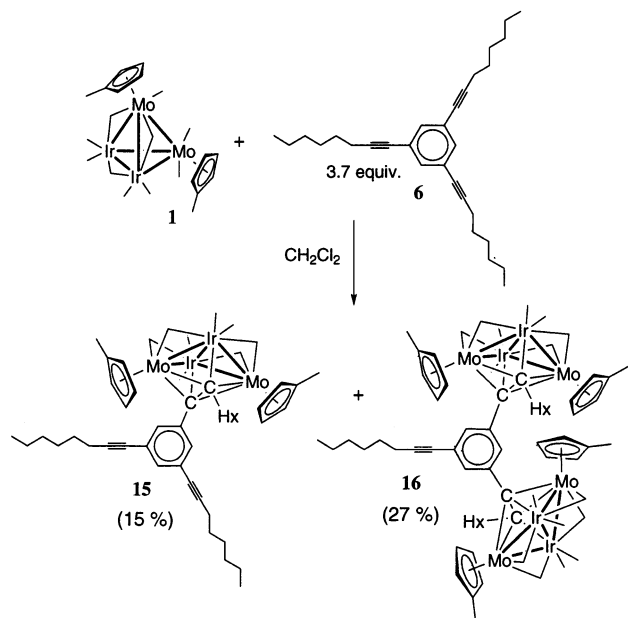
The introduction of cluster units onto 1,3,5-tris(oct-1′-ynyl)benzene (**6**) was attempted in a stepwise manner. The reaction of **1** with an excess (3.7 equiv) of **6** in refluxing dichloromethane, followed by TLC, afforded three green products which were characterized by IR, ^{1}H NMR, and SI mass spectrometry (Scheme 4). The isolated products, all oils or oily solids, were identified

(58) Lucas, N. T.; Humphrey, M. G.; Healy, P. C.; Williams, M. L. *J. Organomet. Chem.* **1997**, *545–546*, 519.

Scheme 3

Scheme 4

as Mo$_2$Ir$_2\{\mu_4$-η^2-Me(CH$_2$)$_5$C$_2$C$_6$H$_3$-3,5-[C≡C(CH$_2$)$_5$Me]$_2\}$-(CO)$_8(\eta^5$-C$_5$H$_4$Me)$_2$ (**15**), [Mo$_2$Ir$_2$(CO)$_8(\eta^5$-C$_5$H$_4$Me)$_2$]$_2$-$\{\mu_8$-η^4-[Me(CH$_2$)$_5$C$_2$]$_2$-1,3-C$_6$H$_3$-5-C≡C(CH$_2$)$_5$Me$\}$ (**16**), and Mo$_2$Ir$_2\{\mu_4$-η^2-Me(CH$_2$)$_5$C$_2$C≡C(CH$_2$)$_5$Me$\}$(CO)$_8(\eta^5$-C$_5$H$_4$Me)$_2$ (**17**). The last-mentioned product, **17**, results from coordination of **1** to Me(CH$_2$)$_5$C≡CC≡C(CH$_2$)$_5$Me, an impurity known to be present in the triyne precursor (see above). The solution IR spectra of the products exhibit the expected ν(CO) pattern, along with a weak band at 2224−2229 cm^{-1} corresponding to a noncoor-

dinated C≡C group. The ^{1}H NMR spectrum of **15** contains resonances at δ 7.07 and 6.89 in a 1:2 ratio, and **16** contains resonances at δ 6.80 and 6.21 in a 2:1 ratio, assigned to the central ring protons. The SIMS spectra of **15** and **17** contain molecular ions and fragments corresponding to stepwise loss of carbonyls; the highest band in the mass spectrum of **16** corresponds to the fragment ion [M − 4CO]$^+$. An attempt was made to introduce a third cluster unit onto the noncoordinated C≡C group of **16**, a mixture of **16** and 2.2 equiv of **1** being heated in refluxing dichloromethane for 4 h; however, the product was unstable, and the spectroscopic data acquired for this product were insufficient to establish its identity.

Coupling of Cluster−Alkyne Adducts To Form π-Delocalized Frameworks. The di- and tricluster complexes described above were synthesized by reaction of **1** or **2** with the preformed di- or triyne. The alternative strategy which was mentioned above is to coordinate functionalized monoynes to a cluster core and then to couple these alkyne-derived building blocks at the functional group to generate the π-delocalized organic framework with clusters intact. In particular, the formation of **12**−**14** suggests that this strategy may offer the route of choice to a corresponding dicluster adduct with clusters at the "outer" C≡C groups. Thus, a THF/triethylamine solution of Mo$_2$Ir$_2\{\mu_4$-η^2-Me(CH$_2$)$_5$C$_2$-4-C$_6$H$_4$I$\}$(CO)$_8(\eta^5$-C$_5$H$_4$Me)$_2$ (**7**) and Mo$_2$Ir$_2\{\mu_4$-η^2-Me-(CH$_2$)$_5$C$_2$-4-C$_6$H$_4$C≡CH$\}$(CO)$_8(\eta^5$-C$_5$H$_4$Me)$_2$ (**9**) was stirred with dichlorobis(triphenylphosphine)palladium(II) and copper(I) iodide catalysts at room temperature for 40 h, to afford [Mo$_2$Ir$_2$(CO)$_8(\eta^5$-C$_5$H$_4$Me)$_2$]$_2\{\mu_8$-η^4-Me(CH$_2$)$_5$C$_2$-4-C$_6$H$_4$C≡CC$_6$H$_4$-4-C$_2$(CH$_2$)$_5$Me$\}$ (**18**) and [Mo$_2$Ir$_2$(CO)$_8$-$(\eta^5$-C$_5$H$_4$Me)$_2$]$_2\{\mu_8$-η^4-Me(CH$_2$)$_5$C$_2$-4-C$_6$H$_4$C≡CC≡CC$_6$H$_4$-4-C$_2$(CH$_2$)$_5$Me$\}$ (**19**), following TLC and crystallization (Scheme 5). The products have been characterized by IR, ^{1}H NMR, and SI mass spectrometry and satisfactory microanalyses, and, in the case of **19**, a single-crystal X-ray structural study. The solution IR spectra exhibit the distinctive ν(CO) pattern for the Mo$_2$Ir$_2$C$_2$ cluster core and are almost identical with each other. The most significant difference in the ^{1}H NMR spectra is in the aromatic ring resonances, doublets at δ 7.30, 7.03 (**18**) and δ 7.31, 7.01 (**19**) being observed. The SIMS spectra of both products contain molecular ions differing by 24 mass units between the two compounds and consistent with the extra C≡C group in **19**.

The desired adduct **18** was isolated as the major product. The minor product **19** results from the homocoupling of two terminal alkyne fragments, viz. **9**. In Sonogashira coupling, the formation of the active catalyst [Pd^0(PPh$_3$)$_2$] from PdCl$_2$(PPh$_3$)$_2$ involves the generation of 1 equiv of homocoupled alkyne,[59] but this does not account for all of the **19** formed. In the presence of an appropriate oxidizing agent (such as O$_2$), the copper-(I) iodide cocatalyst can catalyze the oxidative coupling of two terminal alkyne units.[60] While efforts were made to exclude oxygen from the reaction mixture, only a small amount of adventitious oxygen would be sufficient, over the 40 h period of the reaction, to form the quantity of **19** which was isolated.

(59) Sonogashira, K.; Tohda, Y.; Hagihara, N. *Tetrahedron Lett.* **1975**, *16*, 4467.
(60) Brandsma, L. *Preparative Acetylenic Chemistry*, 2nd ed.; Elsevier: Amsterdam, 1988.

Scheme 5

18
(24 %)

+

19
(8 %)
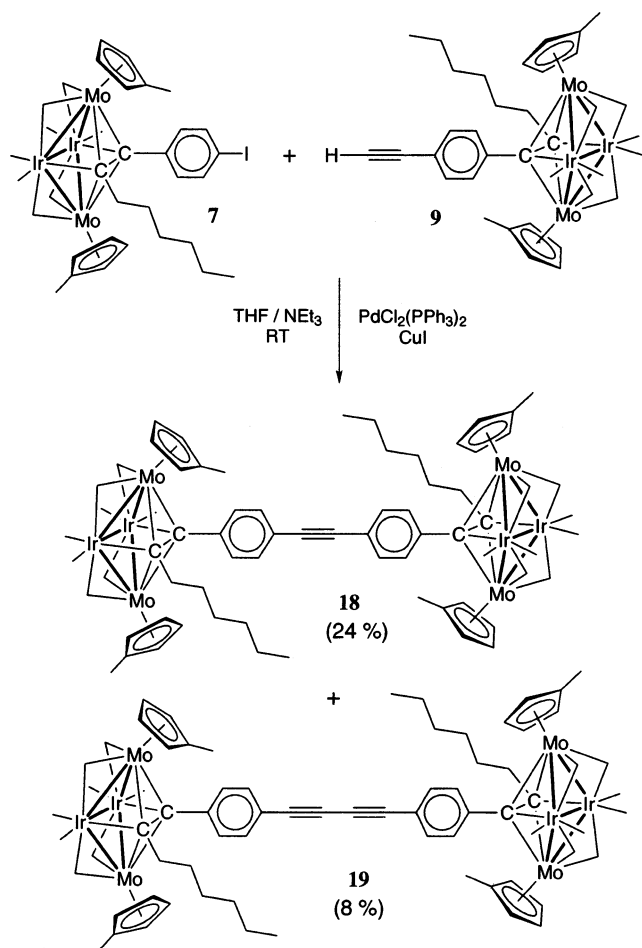
Crystal Structure of 19. The molecular structure of **19**, as determined by a single-crystal X-ray study, is consistent with the formulation given above and confirms the μ_4-η^2-coordination of two of the C≡C groups to Mo_2Ir_2 metal cores, which adopt butterfly geometries. Crystal data for the structural study are summarized in Table 1, and selected bond lengths and angles are listed in Table 2. An ORTEP plot showing the molecular geometry and atomic numbering scheme is shown in Figure 2; the molecule lies on an inversion center, and the symmetry-expanded structure is shown. The iridium atoms form the hinge of the butterfly, each being ligated by two terminal carbonyls; the molybdenum atoms occupy the wingtip sites, and each is ligated by an η^5-methylcyclopentadienyl group. The four remaining carbonyl ligands unsymmetrically bridge the Mo−Ir bonds ($Mo-C_{av} = 2.02$ Å; $Ir-C_{av} = 2.35$ Å). The alkyne ligand bridges all four metals, lying parallel to the Ir1−Ir2 vector and completing a *closo*-octahedral core consisting of the four metals and two "acetylenic" carbon atoms. The Ir−Ir bond length (2.687(1) Å) and Mo−Ir bond lengths (2.789(2)−2.837(2) Å) are consistent with those of the related phenylacetylene adduct $Mo_2Ir_2(\mu_4$-η^2-$HC_2Ph)(\mu$-$CO)_4(CO)_4(\eta^5$-$C_5H_5)_2$.[58] The core carbons C27 and C28 of **19** interact more closely with iridium (Ir−C = 2.09(2)−2.12(2) Å) than with molybdenum (Mo−C = 2.30(2)−2.41(2) Å). The core C27−C28 bond length (1.43(2) Å) falls between single- and double-bond orders. The C36−C36* bond length within the bridge (1.40(3) Å) is typical of the C≡**C**−**C**≡C group. The

C≡C (1.19(2) Å) and other C−C bond lengths within the bridge are also in agreement with typical interatomic distances.[61]

Electrochemical Studies. We have previously reported cyclic voltammetric studies of the monocluster compounds $M_2Ir_2(\mu_4$-η^2-$RC_2Ph)(CO)_8(\eta^5$-$C_5H_4Me)_2$ (R = Ph, M = Mo (**20**), W (**21**); R = Me, M = Mo (**22**), W (**23**)) (which serve as benchmarks for the redox behavior of isolated, noncommunicating, clusters) and the dicluster compounds **10** and **11**.[34] We have now extended this study to embrace some of the di- and tricluster compounds prepared in the current work, the results of these investigations being collected in Table 3. Note that no significant variation to tabulated data was observed upon decreasing the temperature (to 230 K) or increasing the scan rate (to 1600 mV s^{-1}); the listed data were obtained at room temperature (293 K) with a scan rate of 200 mV s^{-1}.

The cyclic voltammograms of **10−14, 18**, and **19** are similar, representative traces (those of **18**, **13**, and **14**, together with that of **22**) being shown in Figure 3. The oxidative behaviors of the compounds using a switching potential of 1.5 V are uniform, with a quasi-reversible (**20**, **21**) or reversible process (F/f, oxidation 1) at less positive potentials, with an irreversible process (G, oxidation 2) at more positive potentials, and with processes F/f and G each probably corresponding to one electron per cluster unit from earlier studies with **20−23**.[34] (Note that the quantification of the number of electrons involved in these processes is by peak height comparison with $[Fe(\eta^5$-$C_5Me_5)_2]/[Fe(\eta^5$-$C_5Me_5)_2]^+$, a known one-electron standard. The (probably) significantly different diffusion coefficients of decamethylferrocene and the present series of clusters suggests that this quantification should be treated with caution.) Oxidation potentials for the former process F/f increase on replacing tungsten with molybdenum (ca. 0.2 V) and on replacing phenyl with an alkyl substituent at the coordinated alkyne. Associated with the irreversible oxidation process G is a reduction process H on the reverse sweep. As was also noted with related phenylenevinylene-linked alkynyl cluster analogues,[34] no difference in oxidative behavior is seen with the present series of compounds in proceeding from monocluster compounds to dicluster compounds.

The single irreversible reduction process (using a switching potential of −1.8 V) noted with "model" compounds **20−23**[34] is also seen with the dicluster compounds **18** and **19** (A, reduction 1), in which the cluster units are linked by $C_6H_4(C≡C)_nC_6H_4$ (n = 1, 2) bridges. In contrast, the dicluster compounds **10**, **11**, and **13**, in which the cluster units are linked by a single phenylene bridge, display two irreversible reduction waves (A, reduction 1; B, reduction 2), and the tricluster compounds **12** and **14**, also containing phenylene-linked cluster units, show three irreversible reduction waves. Associated with the irreversible reduction process A is an oxidation process D on the reverse sweep. Replacing the "model" compound by a phenylene-linked dicluster compound and then the tricluster compound (in proceeding from **22** to **10** and then **12** or **23** to **11/13** and

(61) Allen, F. H.; Kennard, O.; Watson, D. G.; Brummer, L.; Orpen, A. G.; Taylor, R. In *International Tables for Crystallography*; Wilson, A. J. C., Ed.; Kluwer: Dordrecht, The Netherlands, 1992; Vol. C, p 685.

**Table 3. Cyclic Voltammetric Data (V) for Mono-, Di-, and Tricluster Compounds**

| | oxidn 2 | | oxidn 1 | | redn 1 | | redn 2 | | redn 3 | |
| | E_p | $i_{p,c}/i_{p,a}$ | $E_{1/2}$ [E_p^f − E_p^r, mV] | $i_{p,c}/i_{p,a}$ | E_p | $i_{p,a}/i_{p,c}$ | E_p | $i_{p,a}/i_{p,c}$ | E_p | $i_{p,a}/i_{p,c}$ |
compd										
Monocluster Compounds										
$Mo_2Ir_2(\mu_4\text{-}\eta^2\text{-PhC}_2\text{Ph})(CO)_8(\eta^5\text{-C}_5H_4Me)_2$ (**20**)[a]	1.18	irrev	0.80 [60]	0.65	−1.22	irrev				
$W_2Ir_2(\mu_4\text{-}\eta^2\text{-PhC}_2\text{Ph})(CO)_8(\eta^5\text{-C}_5H_4Me)_2$ (**21**)[a]	0.90	irrev	0.58 [60]	0.75	−1.36	irrev				
$Mo_2Ir_2(\mu_4\text{-}\eta^2\text{-MeC}_2\text{Ph})(CO)_8(\eta^5\text{-C}_5H_4Me)_2$ (**22**)[a]	1.19	irrev	0.66 [75]	1	−1.32	irrev				
$W_2Ir_2(\mu_4\text{-}\eta^2\text{-MeC}_2\text{Ph})(CO)_8(\eta^5\text{-C}_5H_4Me)_2$ (**23**)[a]	0.96	irrev	0.45 [74]	1	−1.48	irrev				
Dicluster Compounds										
$[Mo_2Ir_2(CO)_8(\eta^5\text{-C}_5H_4Me)_2]_2\{\mu_8\text{-}\eta^4\text{-Me(CH}_2)_5C_2C_6H_4\text{-}4\text{-C}_2(CH_2)_5Me\}$ (**10**)[a]	1.20	irrev	0.70 [65]	1	−1.22	irrev	−1.44	irrev		
$[W_2Ir_2(CO)_8(\eta^5\text{-C}_5H_4Me)_2]_2\{\mu_8\text{-}\eta^4\text{-Me(CH}_2)_5C_2C_6H_4\text{-}4\text{-C}_2(CH_2)_5Me\}$ (**11**)[a]	0.94	irrev	0.56 [65]	1	−1.26	irrev	−1.52	irrev		
$[W_2Ir_2(CO)_8(\eta^5\text{-C}_5H_4Me)_2]_2\{\mu_8\text{-}\eta^4\text{-Me(CH}_2)_5C_2\text{-}4\text{-C}_6H_4C_2C_6H_4\text{-}4\text{-C}\equiv C(CH_2)_5Me\}$ (**13**)	0.97	irrev	0.55 [65]	1	−1.31	irrev	−1.63	irrev		
$[Mo_2Ir_2(CO)_8(\eta^5\text{-C}_5H_4Me)_2]_2\{\mu_8\text{-}\eta^4\text{-Me(CH}_2)_5C_2\text{-}4\text{-C}_6H_4C\equiv CC_6H_4\text{-}4\text{-C}_2(CH_2)_5Me\}$ (**18**)	1.19	irrev	0.72 [60]	1	−1.28	irrev				
$[Mo_2Ir_2(CO)_8(\eta^5\text{-C}_5H_4Me)_2]_2\{\mu_8\text{-}\eta^4\text{-Me(CH}_2)_5C_2\text{-}4\text{-C}_6H_4C\equiv CC\equiv CC_6H_4\text{-}4\text{-C}_2(CH_2)_5Me\}$ (**19**)	1.20	irrev	0.73 [60]	1	−1.34	irrev				
Tricluster Compounds										
$[Mo_2Ir_2(CO)_8(\eta^5\text{-C}_5H_4Me)_2]_3\{\mu_{12}\text{-}\eta^6\text{-Me(CH}_2)_5C_2\text{-}4\text{-C}_6H_4C_2C_6H_4\text{-}4\text{-C}_2(CH_2)_5Me\}$ (**12**)	1.19	irrev	0.72 [75]	1	−1.04	irrev	−1.19	irrev	−1.42	irrev
$[W_2Ir_2(CO)_8(\eta^5\text{-C}_5H_4Me)_2]_3\{\mu_{12}\text{-}\eta^6\text{-Me(CH}_2)_5C_2\text{-}4\text{-C}_6H_4C_2C_6H_4\text{-}4\text{-C}_2(CH_2)_5Me\}$ (**14**)	0.93	irrev	0.54 [75]	1	−1.15	irrev	−1.43	irrev	−1.65	irrev

[a] Reference 34.

then **14**) results in a progressively increased ease of reduction, as judged by the potential for cathodic reduction 1. Not surprisingly, the behavior of the butadiyne-linked **19** is similar to that for its ethyne-linked analogue **18**.

Computational Studies. To understand the electrochemical behavior of these mono-, di-, and tricluster compounds, approximate density functional theory calculations were carried out on $Mo_2Ir_2(\mu_4\text{-}\eta^2\text{-MeC}_2Ph)$-$(CO)_n(\eta^5\text{-C}_5H_5)_2$ ($n = 7, 8$) in the +1, 0, −1, and −2 charge states. In most instances C_s symmetry was employed, with the mirror plane containing the iridium atoms and the C_2 acetylene moiety of the MeC_2Ph ligand. Initial geometries used featured bridging interactions for four carbonyl ligands with the Mo−Ir bonds, but these ligands were not prevented from adopting terminally coordinated configurations, provided that C_s symmetry was conserved. The remaining (three or four) carbonyl ligands were constrained to lie within the mirror plane and were assumed to be associated exclusively with the iridium atoms, with an Ir−Ir bridging interaction assumed (but not constrained) for one of these ligands in the "carbonyl-deficient" structure ($n = 7$), while all of the four exclusively iridium-coordinated carbonyl ligands in the more highly carbonylated structure ($n = 8$) were assumed to be terminal. While free rotation of either the methyl or the phenyl group about its respective C−C axis was precluded by C_s symmetry constraints, separate calculations were pursued for the two cases in which the phenyl ring was constrained to lie either within, or perpendicular to, the mirror plane. In addition, geometry optimizations for the 0 and −2 charge states were pursued with the phenyl ring initially canted at an angle intermediate between these two cases: the latter calculations were performed in the absence of any symmetry. Relative energies obtained for all of the geometries and charge states investigated are detailed in Table 4.

The orientation of the phenyl ring is most conveniently expressed relative to the plane containing the
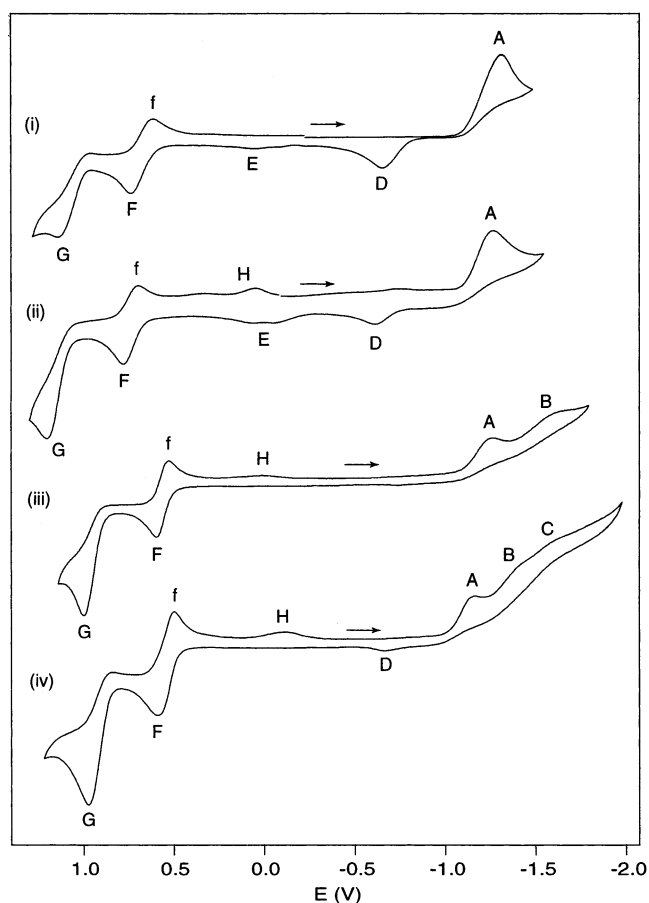
Figure 3. Cyclic voltammograms of (i) 5.8 mM $Mo_2Ir_2(\mu_4\text{-}\eta^2\text{-MeC}_2Ph)(CO)_8(\eta^5\text{-C}_5H_4Me)_2$ (**22**), (ii) 1.0 mM $[Mo_2Ir_2(CO)_8(\eta^5\text{-C}_5H_4Me)_2]_2\{\mu_8\text{-}\eta^4\text{-Me(CH}_2)_5C_2\text{-}4\text{-C}_6H_4C\equiv CC_6H_4\text{-}4\text{-C}_2(CH_2)_5Me\}$ (**18**), (iii) 0.6 mM $[W_2Ir_2(CO)_8(\eta^5\text{-C}_5H_4Me)_2]_2\{\mu_8\text{-}\eta^4\text{-Me(CH}_2)_5C_2\text{-}4\text{-C}_6H_4C_2C_6H_4\text{-}4\text{-C}\equiv C(CH_2)_5Me\}$ (**13**), and (iv) 0.7 mM $[W_2Ir_2(CO)_8(\eta^5\text{-C}_5H_4Me)_2]_3\{\mu_{12}\text{-}\eta^6\text{-Me(CH}_2)_5C_2\text{-}4\text{-C}_6H_4C_2C_6H_4\text{-}4\text{-C}_2(CH_2)_5Me\}$ (**14**) in CH_2Cl_2 with 0.25 M $(NBu^n_4)PF_6$ as supporting electrolyte (scan rate 200 mV s^{-1}).

Table 4. Relative Energies for $Mo_2Ir_2(\mu_4\text{-}\eta^2\text{-}MeC_2Ph)(CO)_8(\eta^5\text{-}C_5H_5)_2$ and $[Mo_2Ir_2(\mu_4\text{-}\eta^2\text{-}MeC_2Ph)(CO)_7(\eta^5\text{-}C_5H_5)_2 + CO]$ Structures in Various Charge States, Obtained from DFT Calculations

charge state	structure	sym	E_{rel}(VWN), eV[a]	E_{rel}(B-LYP + ZORA), eV[b]
0	$Mo_2Ir_2(\mu_4\text{-}\eta^2\text{-}MeC_2Ph)(CO)_8(\eta^5\text{-}C_5H_5)_2$ (in-plane Ph)	C_s	0	0
	$Mo_2Ir_2(\mu_4\text{-}\eta^2\text{-}MeC_2Ph)(CO)_8(\eta^5\text{-}C_5H_5)_2$ (perpendicular Ph)	C_s	0.52	0.54
	$Mo_2Ir_2(\mu_4\text{-}\eta^2\text{-}MeC_2Ph)(CO)_7(\eta^5\text{-}C_5H_5)_2$ (in-plane Ph) + CO	C_s	2.17	1.55
	$Mo_2Ir_2(\mu_4\text{-}\eta^2\text{-}MeC_2Ph)(CO)_8(\eta^5\text{-}C_5H_5)_2$	none	−0.13	−0.02
−2	$Mo_2Ir_2(\mu_4\text{-}\eta^2\text{-}MeC_2Ph)(CO)_8(\eta^5\text{-}C_5H_5)_2$ (in-plane Ph)	C_s	−2.97	−0.45
	$Mo_2Ir_2(\mu_4\text{-}\eta^2\text{-}MeC_2Ph)(CO)_8(\eta^5\text{-}C_5H_5)_2$ (perpendicular Ph)	C_s	−2.48	0.02
	$Mo_2Ir_2(\mu_4\text{-}\eta^2\text{-}MeC_2Ph)(CO)_7(\eta^5\text{-}C_5H_5)_2$ (in-plane Ph) + CO	C_s	−1.58	−0.10
	$Mo_2Ir_2(\mu_4\text{-}\eta^2\text{-}MeC_2Ph)(CO)_8(\eta^5\text{-}C_5H_5)_2$	none	−2.95	−0.38
+1	$Mo_2Ir_2(\mu_4\text{-}\eta^2\text{-}MeC_2Ph)(CO)_8(\eta^5\text{-}C_5H_5)_2$ (in-plane Ph)	C_s	7.44	6.35

[a] Total bond energy (expressed relative to $Mo_2Ir_2(\mu_4\text{-}\eta^2\text{-}MeC_2Ph)(CO)_8(\eta^5\text{-}C_5H_5)_2$ with the Ph moiety lying in the plane of symmetry) obtained from LDA + VWN geometry optimization calculations using a type II basis set. [b] Relative energy obtained from B-LYP + ZORA single-point calculations using a type IV basis set.

phenyl ipso carbon, the adjacent "acetylenic" carbon atom, and the iridium atom bonded to this "acetylenic" carbon. In calculations featuring C_s symmetry, these three atoms lie within the structure's mirror plane, and the $\angle C_o C_i C\equiv Ir$ dihedral angles (where C_o is one or other of the phenyl's ortho carbons) are either 0 and 180°, indicating that the phenyl ring is coplanar with the mirror plane, or (approximately) ±90°, for a phenyl ring perpendicular to the mirror plane. For both the 0 and −2 charge states, geometry optimizations on both of these phenyl configurations indicate that the "in-plane" configuration is significantly favored relative to the "perpendicular" orientation, with an energy difference of around 0.5 eV between the two orientations. This trend is supported by further calculations in which no symmetry was imposed, thus allowing free rotation of the phenyl group (as well as unsymmetrical relaxation of the rest of the structure): although in such calculations the phenyl adopts neither a coplanar nor a perpendicular configuration, it is markedly closer to the coplanar structure, with $-C_o C_i C\equiv Ir$ dihedrals of +29 and −152° for the neutral charge state and +25 and −156° for the dianion (the neutral cluster's calculated dihedral values can also be very favorably compared to the crystallographic values of +26° and −158°).[34,62] The energy differences between these unsymmetrical structures and the "coplanar" C_s geometries for both the 0 and −2 charge states are also comparatively small, with differences of only 0.13 and −0.02 eV, respectively. Finally, it is also worth noting that the unsymmetrical orientation of the phenyl ring, in either the 0 or −2 charge state, has very little apparent impact on the rest of the cluster's structure: there is very little discernible shift in the orientation of the cyclopentadienyl ligands, or of the various carbonyls, in going from the "coplanar" C_s geometry to the "canted" unsymmetrical structure.

For these reasons, we have largely restricted our calculations on other charge states, or on carbonyl-depleted structures, to such coplanar configurations so as to economize on computational resources.

One surprising result was that, in the −2 charge state calculations on $Mo_2Ir_2(\mu_4\text{-}\eta^2\text{-}MeC_2Ph)(CO)_8(\eta^5\text{-}C_5H_5)_2$, C−C bond formation was seen between the two iridium-ligated carbonyls coordinated trans to the acetylene subunit. This somewhat counterintuitive result occurred spontaneously and was seen to be quite independent of the imposed molecular symmetry or of the orientation of the phenyl moiety. Efforts to obviate this OC−CO linkage, by defining different initial orbital occupations, did not reveal any lower-lying structures lacking this feature. Further calculation with a larger basis set ("type IV", of triple-ζ quality and with smaller frozen cores on Ir {4d} and Mo {3d}) also demonstrated this tendency toward OC−CO linkage, while implementation of nonlocal (B-LYP) corrections to the exchange and correlation functionals did not lead to this feature. It appears, therefore, that this phenomenon is an artefact of the level of theory (local density approximation, including the VWN correlation functional) employed in the majority of our DFT calculations. This apparently spurious result for the dianionic species contrasts with the very good performance of LDA calculations in no-symmetry calculations on the neutral complex,[63] as well as the generally good performance of LDA on other broadly similar systems.[33,55] There was no tendency seen, in any of our calculations on the 0, +1, and −1 charge states, for OC−CO bond formation in this fashion.

Other structural effects of interest include the increasing stability, upon reduction, of an Ir−Ir bridging carbonyl interaction upon carbonyl loss. Such a bridge is stable (according to our calculations) for the −2 charge

---

(62) Agreement between the calculated and experimental bond lengths is also generally very good. While there are no discrepancies as large as 0.1 Å, it appears that our calculations systematically overestimate metal−metal bond lengths by ~0.04−0.05 Å, while underestimating the bonds from molybdenum to the "acetylenic" carbon atoms by ~0.05−0.07 Å. Our "acetylenic" C−C bond length itself is ~0.02 Å too long, while the bonds from these carbons to the methyl and phenyl groups are underestimated by a similar extent. In contrast, B-LYP optimizations performed using the type II basis set deliver a modest improvement in the C−C≡C−C bond lengths, at the expense of substantial overestimation of all of the metal−metal and metal−carbon (alkyne) bond lengths as assessed against crystallographic values. The agreement between B-LYP, VWN, and crystallographic structures regarding the preferred out-of-plane orientation of the phenyl group is excellent, strongly suggesting that this is a consequence of steric crowding around the Ir_2C_2 four-membered ring rather than a crystal-packing effect.

(63) Some comparison of the overall quality of the VWN/type II geometries, versus those obtained via B-LYP with a type II basis set, can be afforded from relativistically corrected, single-point B-LYP + ZORA/type IV basis set calculations on the two sets of geometries. Such a comparison, which has been performed for the neutral and dianionic "in-plane" octacarbonyl structures, as well as for the unsymmetrical neutral geometry, consistently yield B-LYP + ZORA/type IV total energies for the VWN optimized structures which are ~0.4 eV below those for the analogous B-LYP optimized geometries. Interestingly, this result—that the VWN geometries give lower total energies in subsequent B-LYP + ZORA/type IV single-point calculations—holds true even for the dianion structure which, according to VWN (but not B-LYP), features an improbable OCCO ligand. We conclude that, notwithstanding the apparently erroneous OC−CO linkage in the dianionic calculations, VWN yields consistently better overall optimized geometries for these clusters than does B-LYP.

state but not in the neutral cluster (for which terminal coordination of the trans CO, to one of the two iridium atoms, is preferred over a bridging interaction). Furthermore, CO loss from the dianion is a less energetically demanding process than from the neutral cluster, as shown by our relative energies from both the LDA geometry optimizations and the ZORA-corrected B-LYP single-point calculations. We also find that the two-electron reduction process is sufficiently exothermic to liberate one carbonyl ligand from the dianion, and such a process may well account for the observation that electrochemical reduction is irreversible. Finally, calculations have also shown that the "perpendicular phenyl" orientation is disfavored over the "coplanar" configuration, to comparable extents for both the heptacarbonyl cluster and the octacarbonyl cluster.

Discussion. We have previously reported the facile construction of di- and tricluster compounds in which the cluster modules are linked by phenylenevinylene bridges. The present study extends this work to related examples linked by phenyleneethynylene bridges. Our earlier report contrasted the two approaches to constructing such compounds, viz. adding cluster units to preformed organic diynes or coupling appropriately functionalized cluster–alkyne complexes, the former approach proving the more successful. In the present studies, the availability of additional alkyne sites in the bridging group has afforded the possibility of isomers and polycluster arrays from the former approach, and the two synthetic approaches more clearly complement each other: whereas reaction of bis{4-(oct-1′-ynyl)phenyl}ethyne (**5**) with $W_2Ir_2(CO)_{10}(\eta^5-C_5H_4Me)_2$ (**2**) afforded the "1,2-isomer" $[W_2Ir_2(CO)_8(\eta^5-C_5H_4Me)_2]_2$-$\{\mu_8-\eta^4-Me(CH_2)_5C_2-4-C_6H_4C_2C_6H_4-4-C\equiv C(CH_2)_5Me\}$ (**13**) together with the tricluster adduct $[W_2Ir_2(CO)_8(\eta^5-C_5H_4-Me)_2]_3\{\mu_{12}-\eta^6-Me(CH_2)_5C_2-4-C_6H_4C_2C_6H_4-4-C_2(CH_2)_5-Me\}$ (**14**), combining $Mo_2Ir_2\{\mu_4-\eta^2-Me(CH_2)_5C_2-4-C_6H_4I\}$-$(CO)_8(\eta^5-C_5H_4Me)_2$ (**7**) with $Mo_2Ir_2\{\mu_4-\eta^2-Me(CH_2)_5C_2-4-C_6H_4C\equiv CH\}(CO)_8(\eta^5-C_5H_4Me)_2$ (**9**) gave the "1,3-isomer" $[Mo_2Ir_2(CO)_8(\eta^5-C_5H_4Me)_2]_2\{\mu_8-\eta^4-Me(CH_2)_5C_2-4-C_6H_4C\equiv CC_6H_4-4-C_2(CH_2)_5Me\}$ (**18**). The latter reaction necessitated functional group transformations on cluster–alkyne adducts, the Sonogashira coupling in the present studies complementing coupling of the phos-phonate ester anion with aldehyde (on preformed cluster–alkynes) demonstrated in our earlier report. The latter reaction has also suggested a facile route to buta-diyne-linked dicluster complexes, by homocoupling of terminal alkyne-functionalized cluster complexes. Steric factors appear to govern the extent of cluster addition to preformed triynes; while we were not able to add a third cluster unit to $[Mo_2Ir_2(CO)_8(\eta^5-C_5H_4Me)_2]_2\{\mu_8-\eta^4-[Me(CH_2)_5C_2]_2-1,3-C_6H_3-5-C\equiv C(CH_2)_5Me\}$ (**16**), our earlier study demonstrated facile formation of the tricluster compound $[Mo_2Ir_2(\mu-CO)_4(CO)_4(\eta^5-C_5H_4Me)_2]_3\{\mu_{12}-\eta^6-1,3,5-C_6H_3[(E)-CH\equiv CHC_6H_4-4′-C_2(CH_2)_5Me]_3\}$, in which the "arms" are lengthened by additional phenylenevi-nylene groups.

The electrochemical behaviors of the current series of phenyleneethynylene-linked di- and tricluster compounds are essentially the same as those of their phenylenevinylene-linked analogues.[34] In our earlier report, the identity of the redox products was unknown, although a reversible one-electron oxidation (quantified by comparison to an internal decamethylferrocene standard) and irreversible reduction (suggested as two-electron in nature by peak height comparison) were identified; LDA calculations in the present work suggest that the +1 and −2 charge states retain the pseudooctahedral core geometry of the resting state but that two-electron reduction likely proceeds with loss of carbonyl, consistent with the electrochemical irreversibility of this process.

Supporting Information Available: Tables giving X-ray crystallographic data for **19**; data are also available as electronic files in CIF format. This material is available free of charge via the Internet at http://pubs.acs.org.

OM020910K